Diffraction in hadronic collisions

With focus on the ep/eA at EIC

Anna Staśto

PennState
Eberly College of Science

NCBJ, May 23, 2022

Outline

Lecture 1: introduction, diffraction in QCD, HERA measurements

Lecture 2: prospects at EIC: proton tagging capabilities, reduced cross section and DPDFs, longitudinal diffractive structure function, elastic vector meson production in ep/eA

Focus will be on ep/eA. Not pp.

EIC White paper 1212.1701

EIC Yellow Report, 2103.05419

Armesto, Newman, Słomiński, Staśto 1901.09076, 2112.06839

Frankfurt, Guzey, Staśto, Strikman 2203.12289

Diffractive kinematics in DIS

Standard DIS variables:

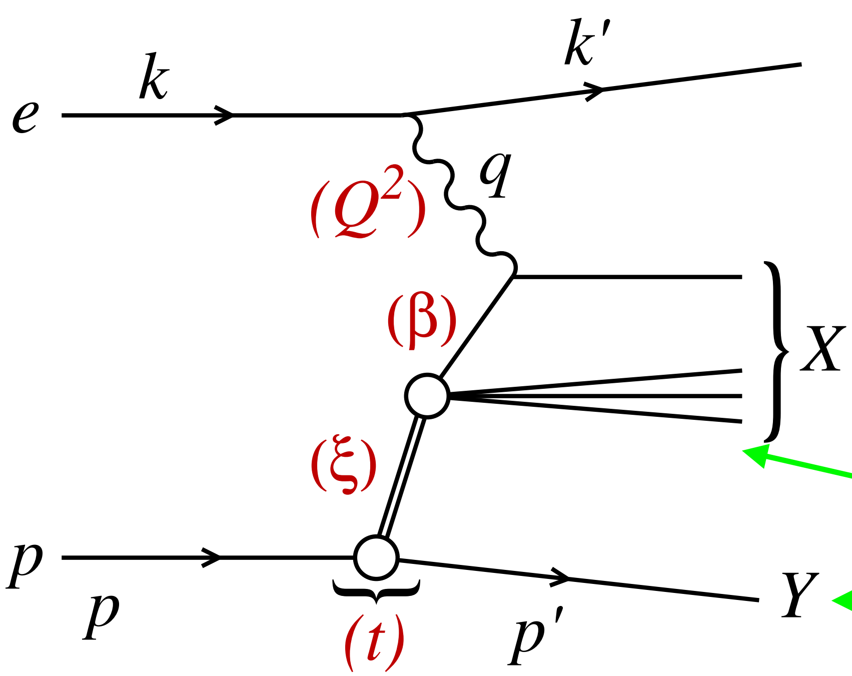

Rapidity gap

electron-proton cms energy squared:

$$s = (k+p)^2$$

photon-proton cms energy squared:

$$W^2 = (q+p)^2$$

inelasticity

$$y = \frac{p \cdot q}{p \cdot k}$$

Bjorken x

$$x = \frac{-q^2}{2p \cdot q}$$

(minus) photon virtuality

$$Q^2 = -q^2$$

Target is scattered elastically: elastic scattering

It can also dissociate into a state Y with the same quantum numbers, but still separated from the rest of particles

Diffractive DIS variables:

$$x = \xi\beta$$

$$\xi \equiv x_{IP} = \frac{Q^2 + M_X^2 - t}{Q^2 + W^2}$$

momentum fraction of the Pomeron w.r.t hadron

$$\beta = \frac{Q^2}{Q^2 + M_X^2 - t}$$

momentum fraction of parton w.r.t Pomeron

$$t = (p - p')^2$$

4-momentum transfer squared

Diffractive cross section, structure functions

Diffractive cross section depends on 4 variables (ξ,β,Q^2,t):

$$\frac{d^4\sigma^D}{d\xi d\beta dQ^2 dt} = \frac{2\pi\alpha_{\rm em}^2}{\beta Q^4} Y_+ \, \sigma_{\rm r}^{\rm D(4)}(\xi,\beta,Q^2,t)$$

$$Y_+ = 1 + (1-y)^2$$

Reduced cross section depends on two structure functions:

$$\sigma_{\rm r}^{\rm D(4)}(\xi,\beta,Q^2,t) = F_2^{\rm D(4)}(\xi,\beta,Q^2,t) - \frac{y^2}{Y_+} F_L^{\rm D(4)}(\xi,\beta,Q^2,t)$$

Upon integration over t:

$$F_{2,L}^{\rm D(3)}(\xi,\beta,Q^2) = \int_{-\infty}^{0} dt \, F_{2,L}^{\rm D(4)}(\xi,\beta,Q^2,t)$$

Dimensions:

$[\sigma_{\rm r}^{\rm D(4)}] = {\rm GeV}^{-2}$

$\sigma_{\rm r}^{\rm D(3)}$ Dimensionless

Measurement methods: LRG vs LP

Large Rapidity Gap method:
request a large rapidity gap (ex. ZEUS 2009 $\xi<0.02$)

Proton Tagging (Leading Proton) method:
detection of a leading proton (ex. Leading Proton Spectrometer in ZEUS, Forward Proton Spectrometer in H1, can go to higher $\xi<0.1$)

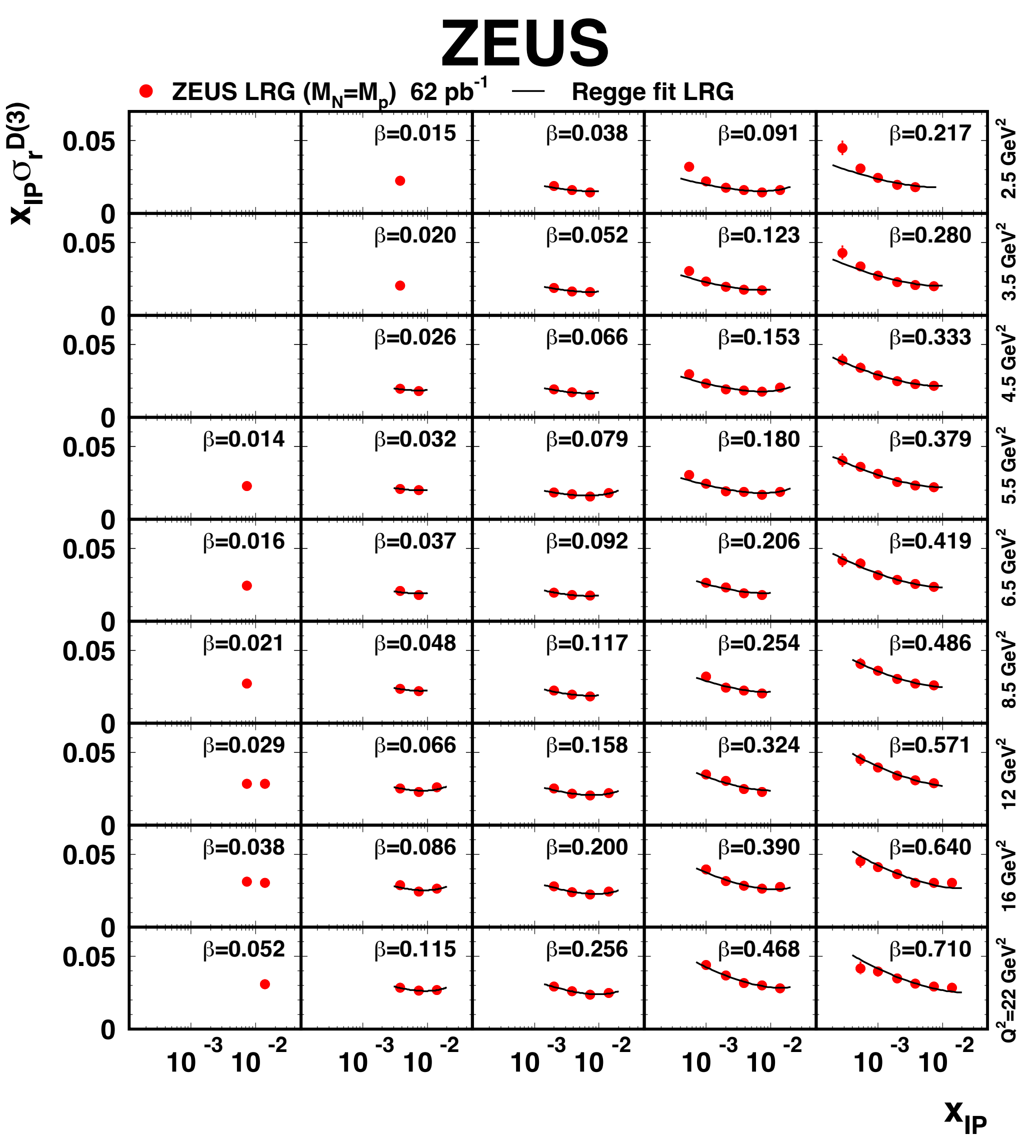

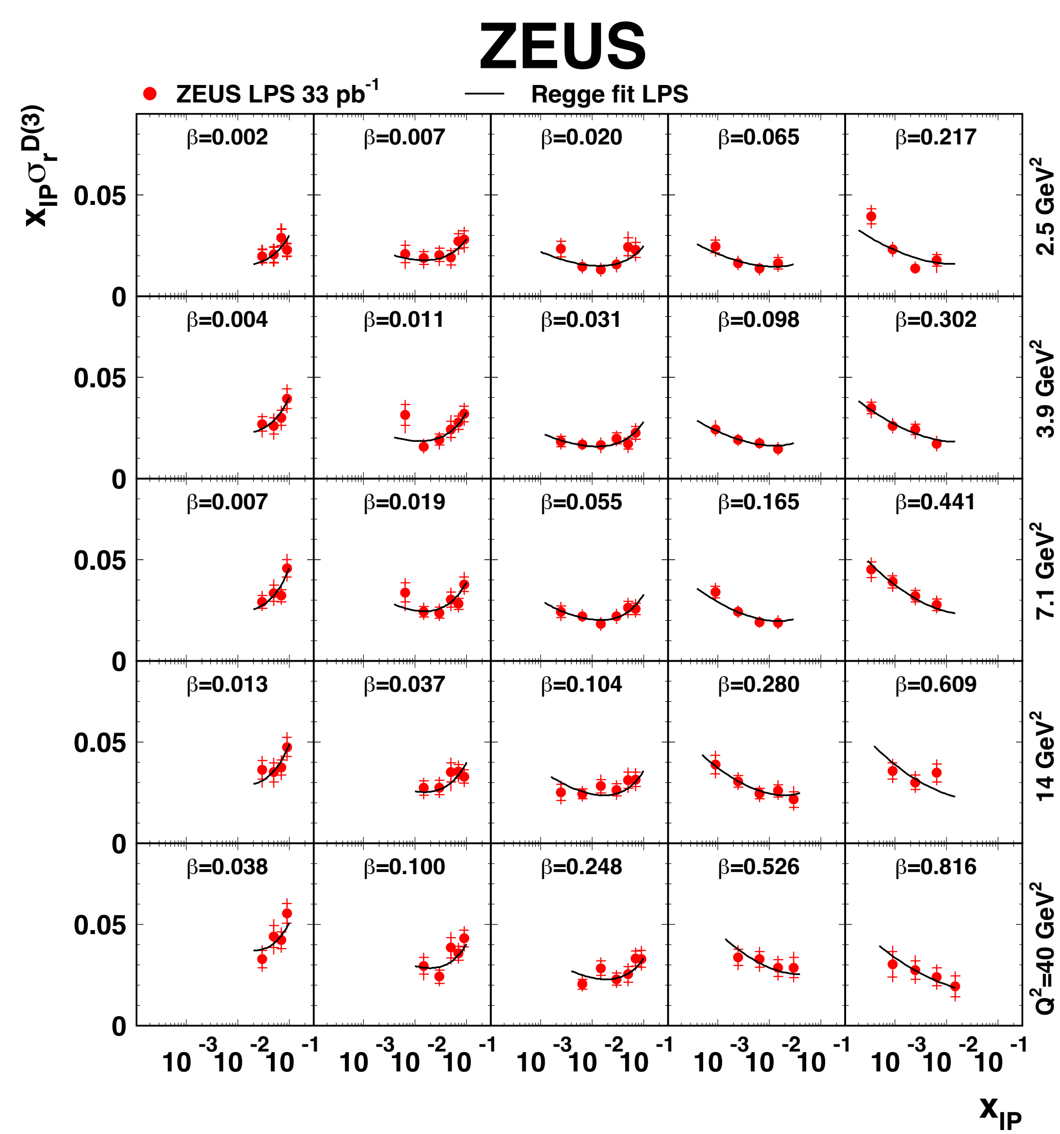

Phase space (x,Q^2) EIC–HERA

EIC can operate at various energy combinations

Can cover wide range of x

Large instantaneous luminosity

Statistics should not be a limiting factor

EIC 3 scenarios - HERA

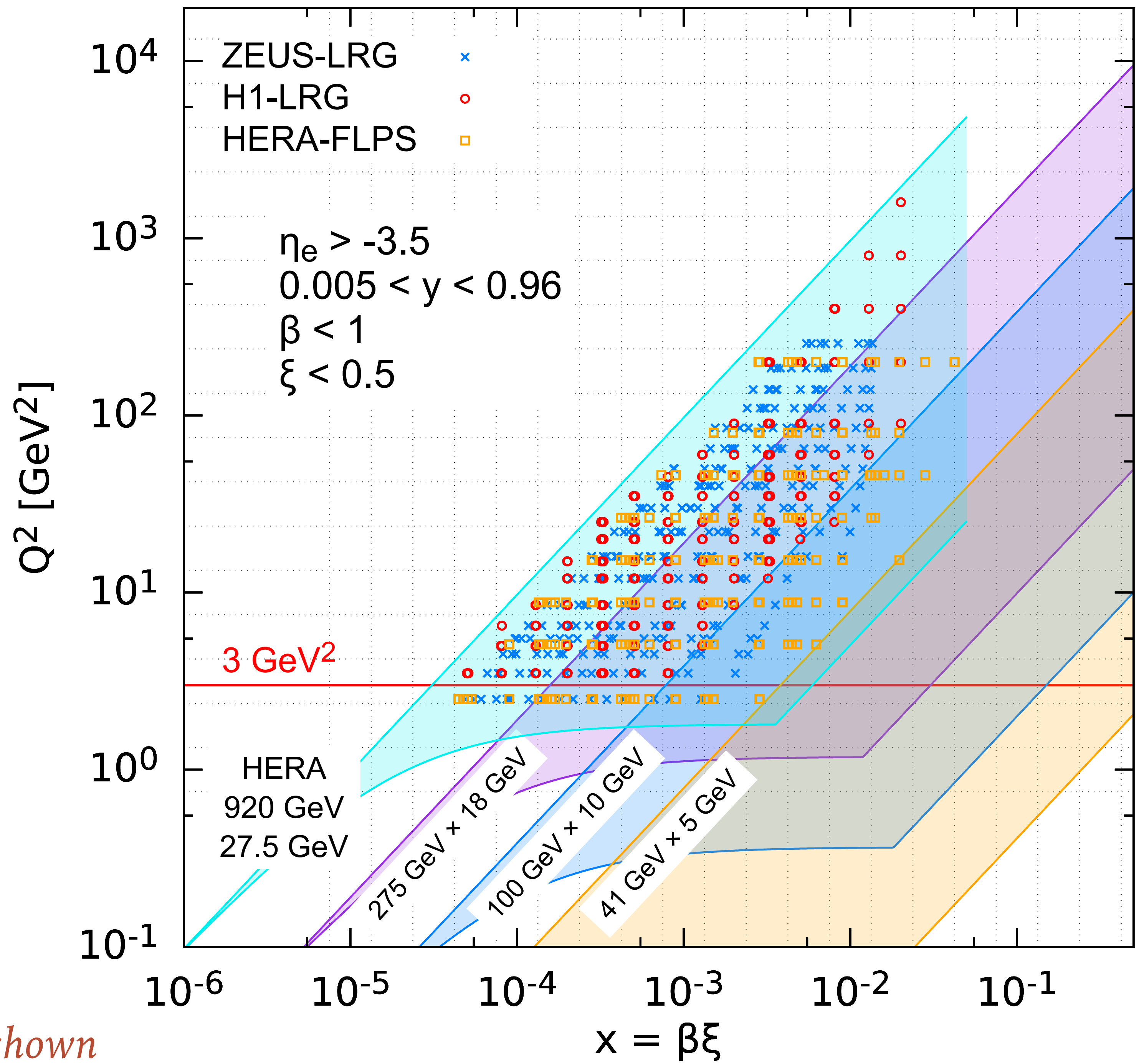

Only selected energy scenarios at EIC shown

Far forward detectors at EIC

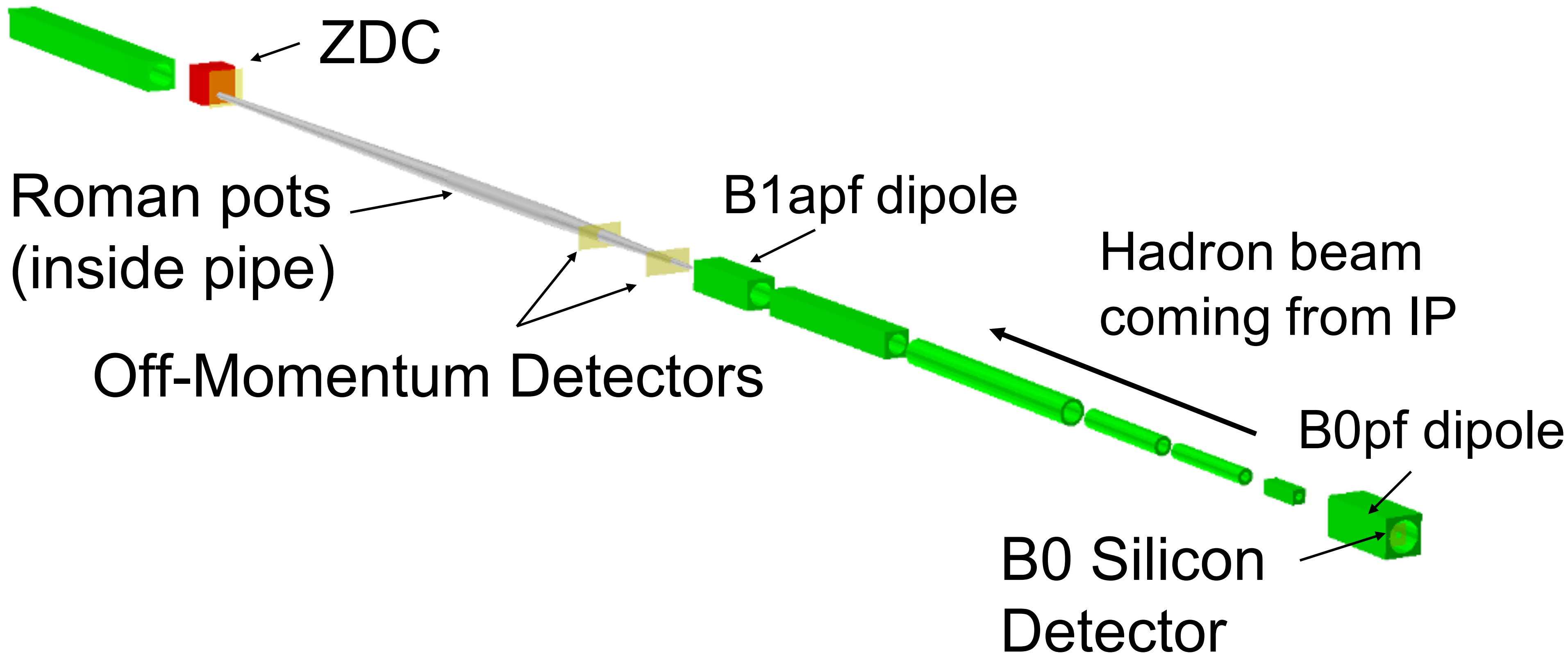

Detector	Angle	Position [m]
ZDC	θ<5.5 mrad	37.5
Roman Pots	0.5<θ<5.0 mrad	26.0, 28.0
Off-momentum detectors	θ<5.0 mrad	22.5, 25.5
B0	6.0<θ<20.0 mrad	5.4<z<6.4

Final proton tagging

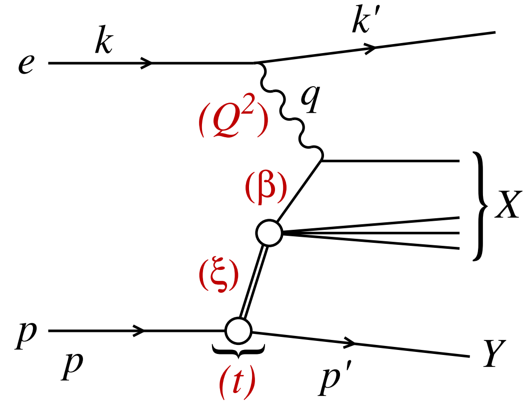

Small angle acceptance i.e. Roman pots

$(x_L, p_\perp, \theta)$ measured in LAB, collinear (e,p) frame

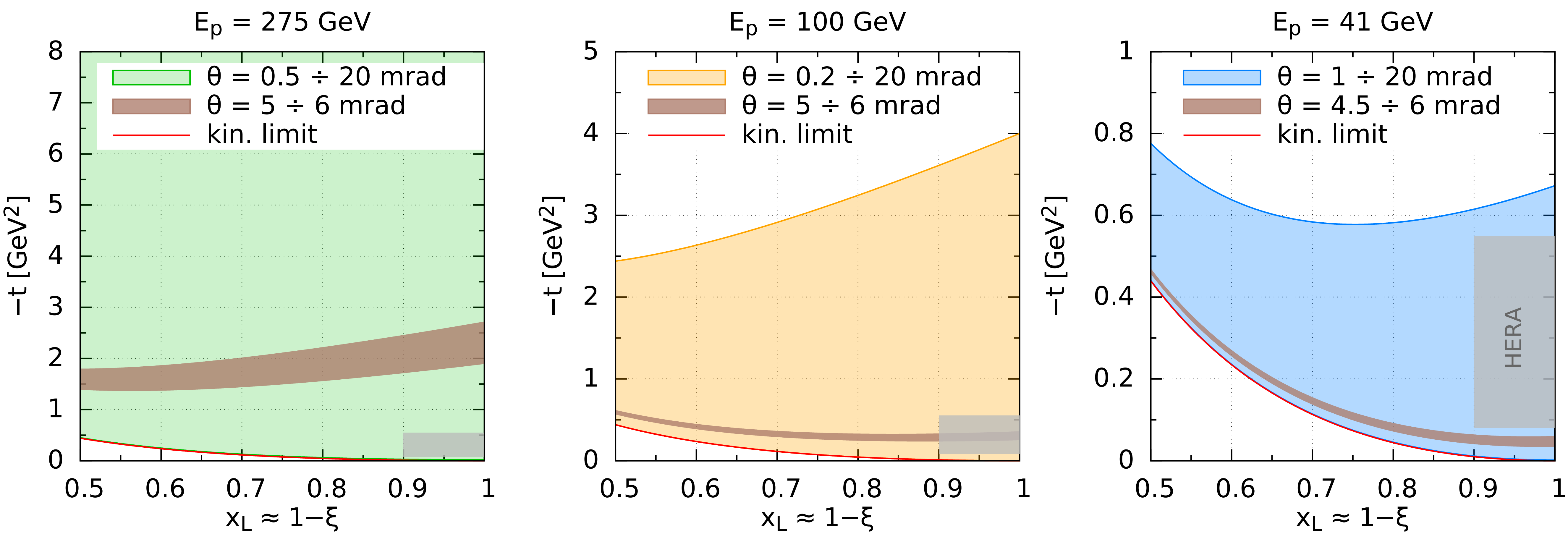

Much better than at HERA

Best way to select diffractive events through proton tagging

$$t = -\frac{p_\perp^2}{x_L} - \frac{(1-x_L)^2}{x_L} m_p^2$$

Resolution study for 18 GeV x 275 GeV

Using RAPGAP to simulate diffraction.

Excellent resolution for variables (x, y, Q^2, β, ξ)

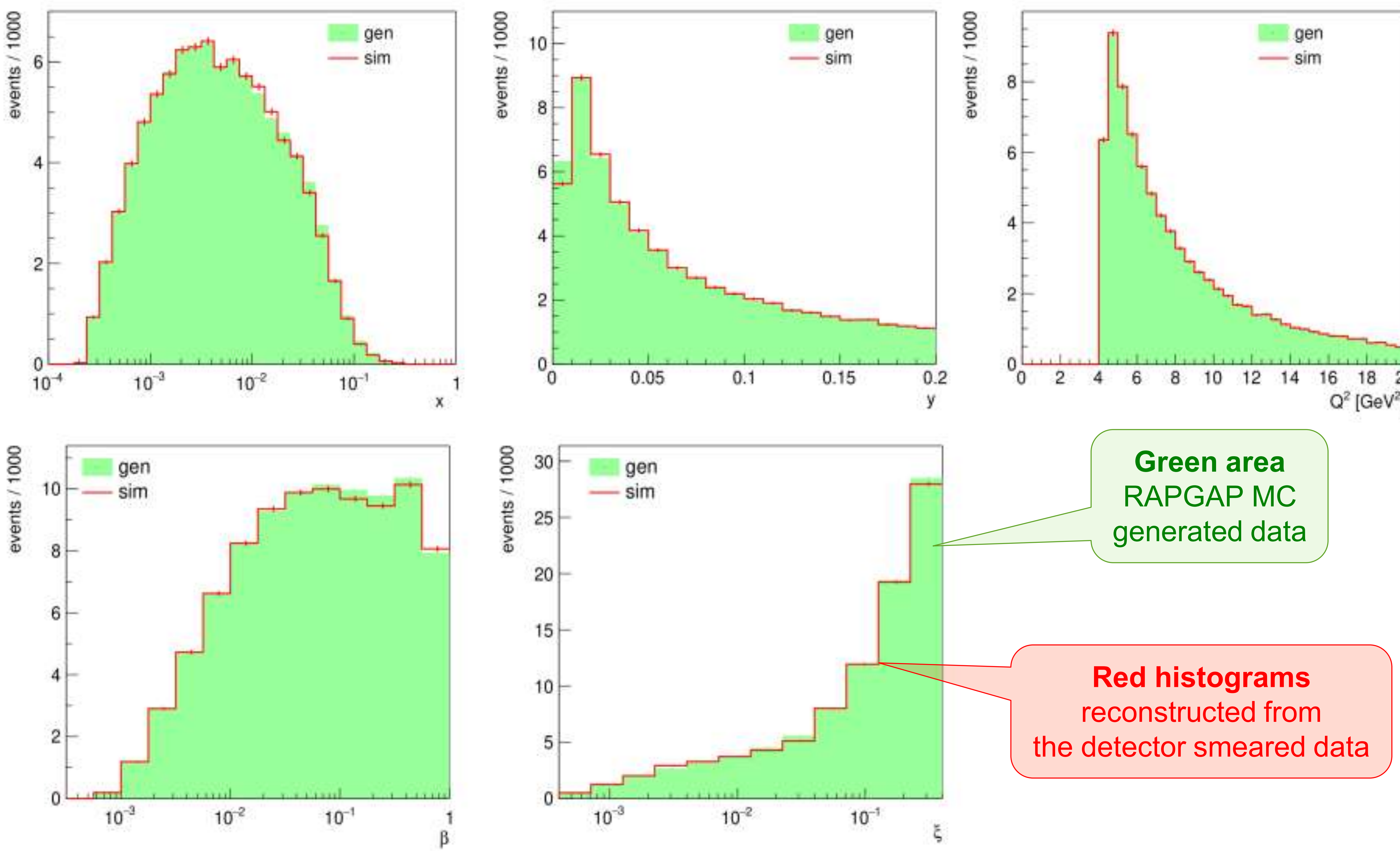

DIS2021 - Wojtek Słomiński - Jagiellonian University 5

Resolution and acceptance

18 GeV x 275 GeV

$$(x_L, p_\perp, t)$$

Generator level

After passing through detector simulation

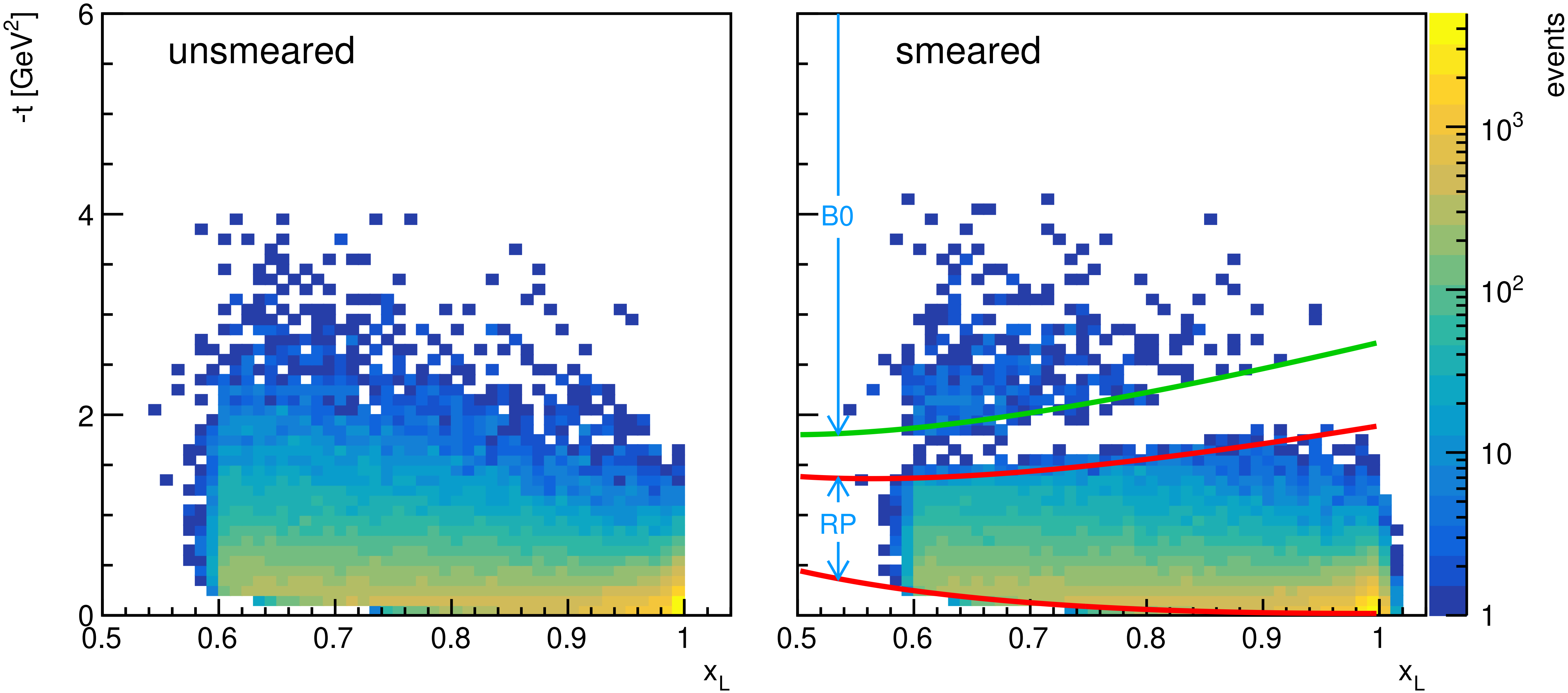

Pseudorapidity distribution

18 GeV x 275 GeV

Green histogram: generated from RAPGAP

Red histogram: reconstructed from smeared data

Hadronic calorimetry up to η<3.5

EM calorimetry up to η<4.5

Use of B0 or other dedicated veto detectors could extend this region

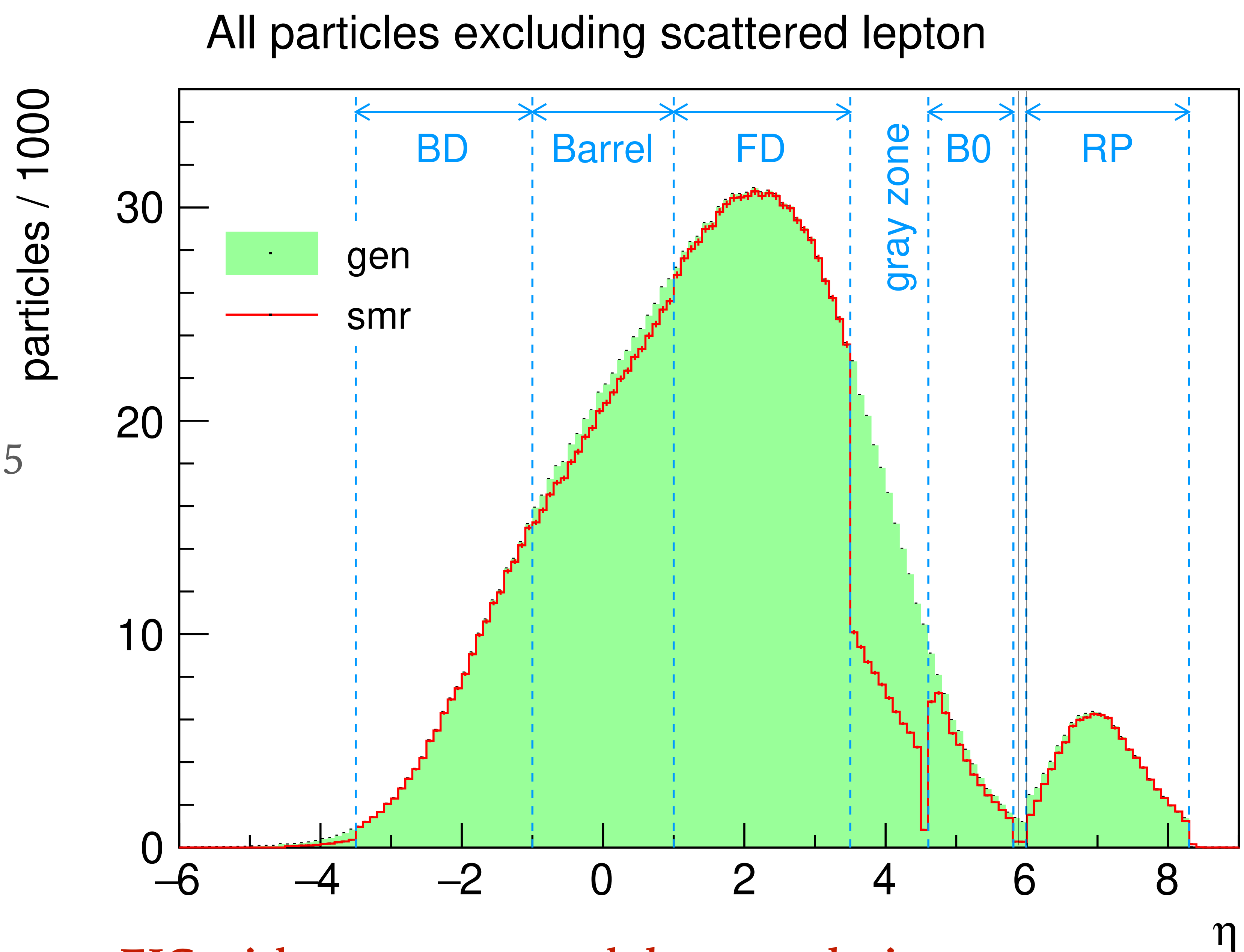

Rapidity gap method challenging at EIC with current central detector design

Leading proton method seems preferred at EIC thanks to excellent forward instrumentation

Pseudodata generation for $\sigma^{D(3)}$

Pseudodata generation

Binning

4 bins per order of magnitude in each β, Q^2, ξ

Simulations

Cross section extrapolation from ZEUS-SJ diffractive PDFs

Random smearing with $\delta_{sys}=5\%$ and δ_{stat} from 10 fb^{-1} integrated luminosity

Several random samples are generated

Fits of diffractive PDFs to $\sigma_r^{D(3)}$

9 parameters to be fitted, standard fit, Fit S

4 remaining parameters, $B_{P/R}$, $\alpha'_{P/R}$ fixed from other measurements

Option: constant gluon density at $\mu_0^2=1.8$ GeV^2 , $B_g=C_g=0$, Fit C with 7 parameters

Pseudodata for $\sigma^{D(3)}$ at EIC

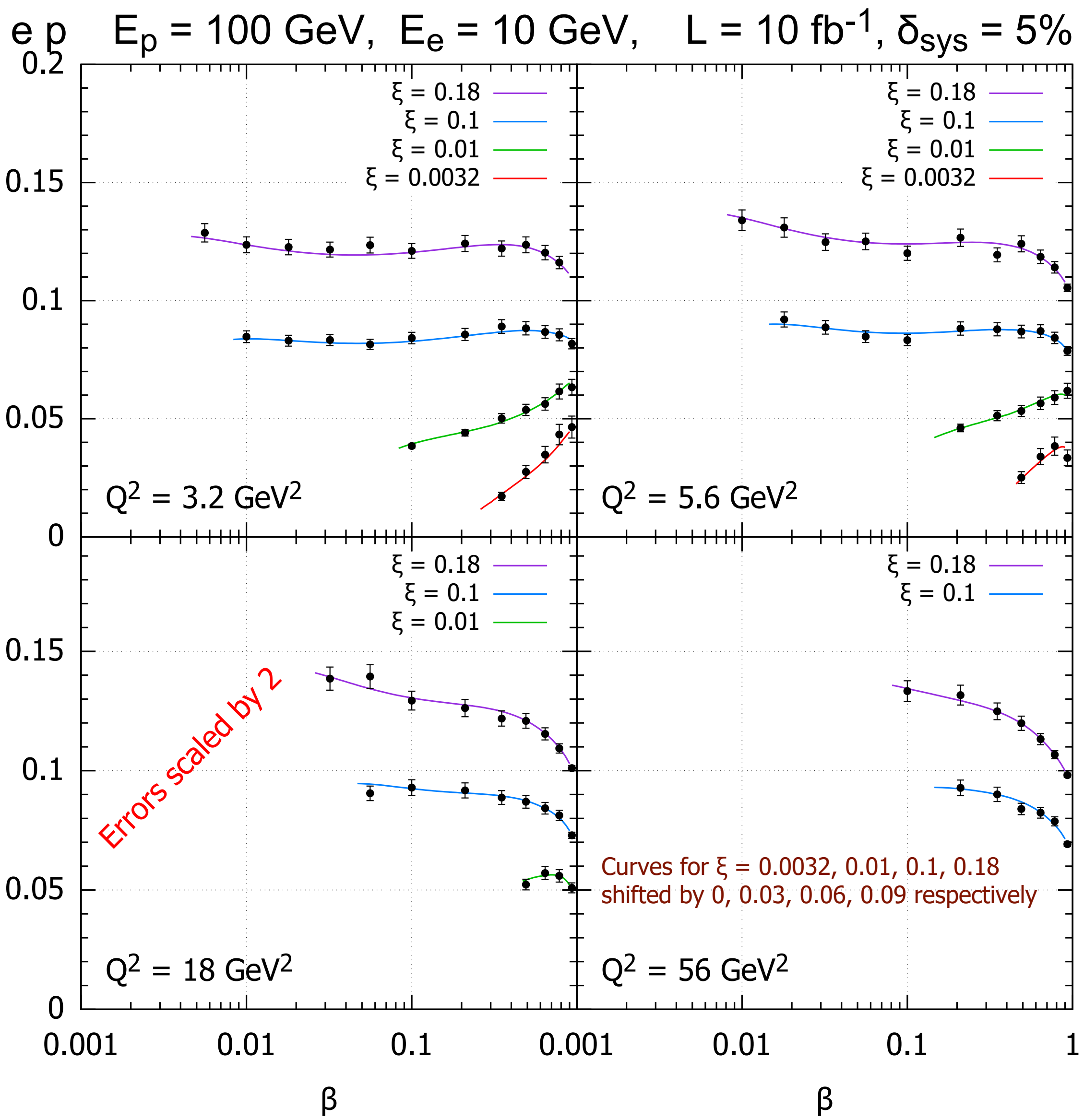

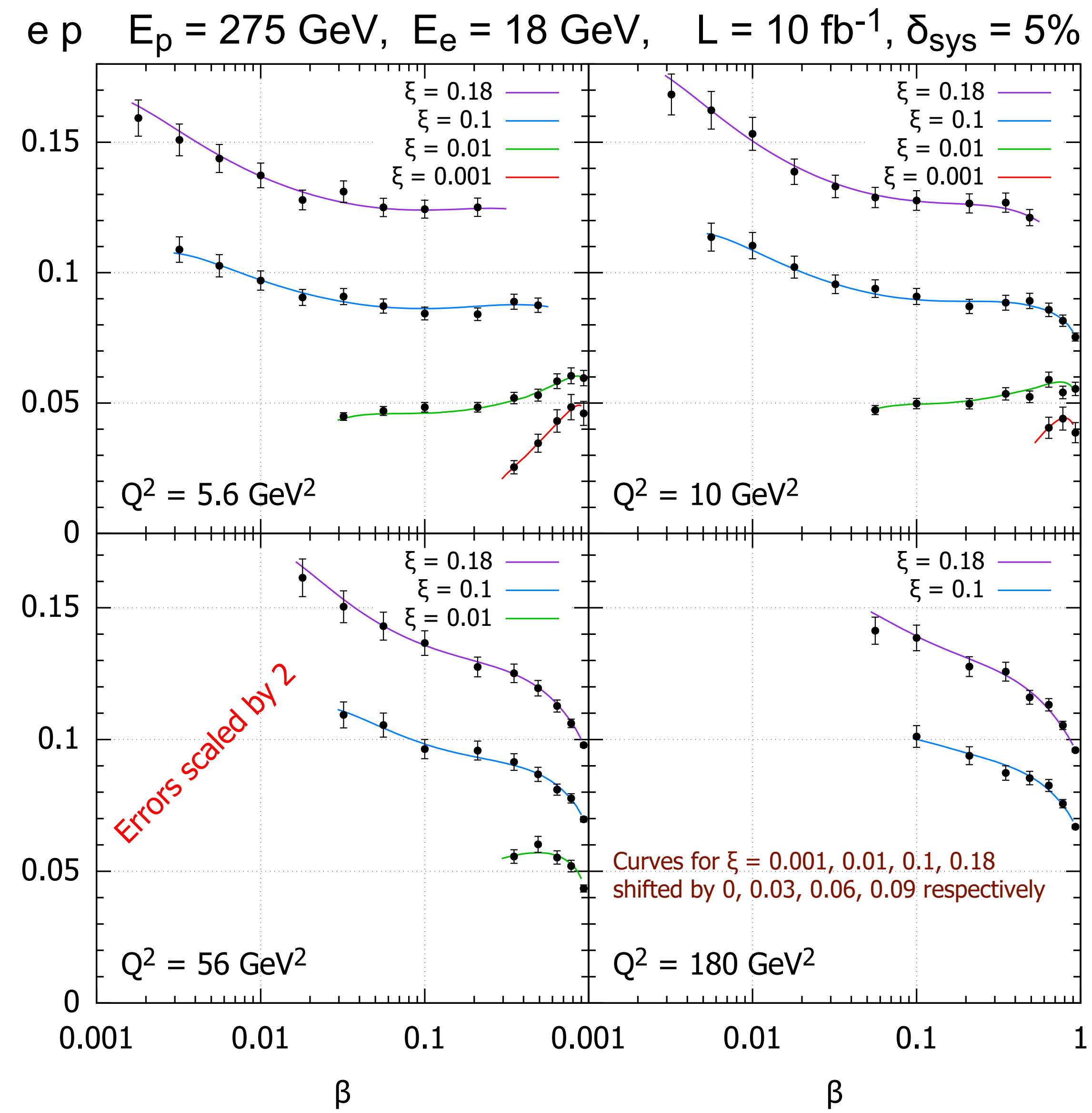

In total:
482 points for $1.3 < Q^2 < 1330\ \mathrm{GeV}^2$

In total:
792 points for $1.3 < Q^2 < 4220\ \mathrm{GeV}^2$

Diffractive PDFs from fits to 18 GeV x 275 GeV data

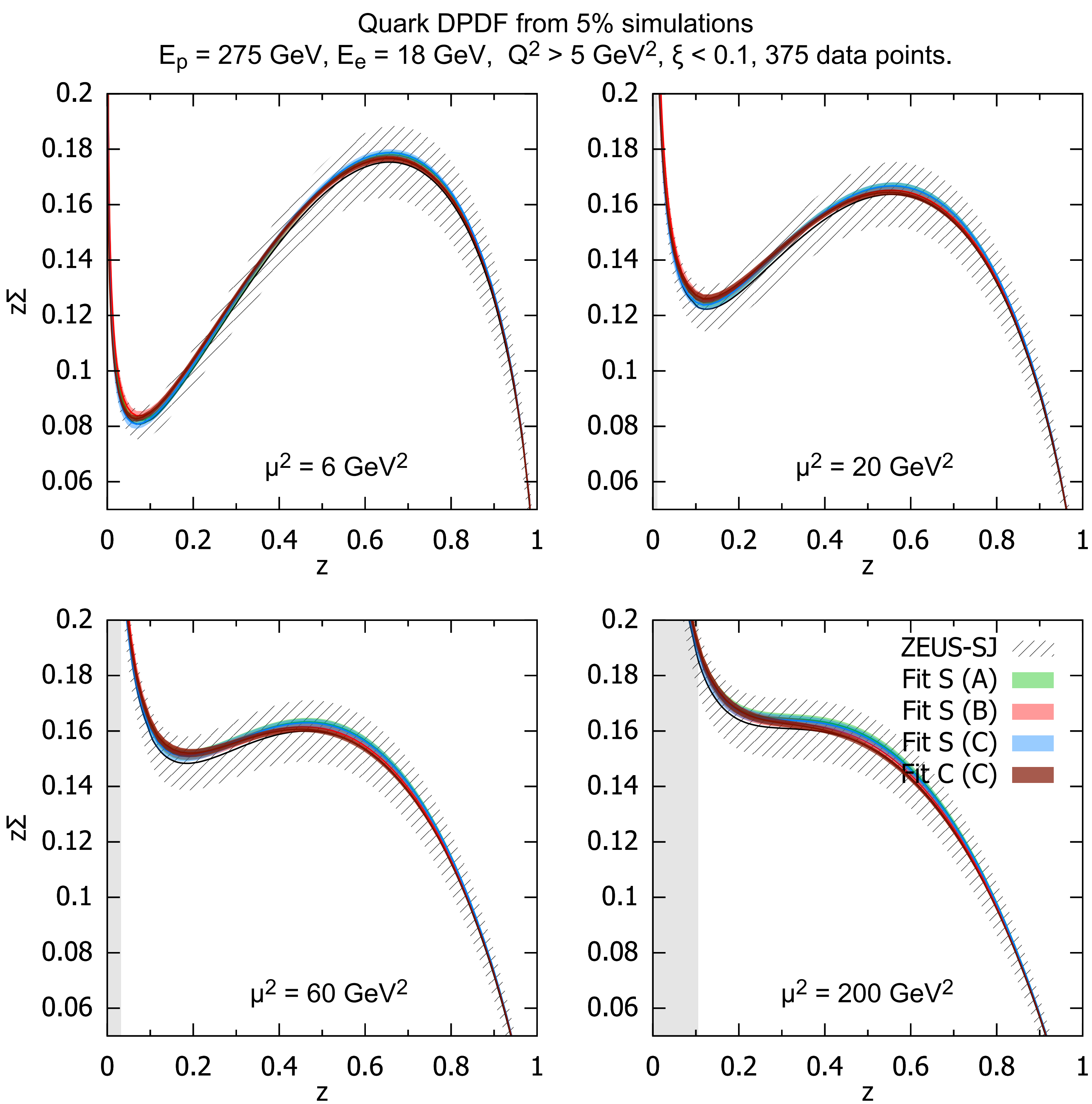

Quark diffractive PDF

Fit S: 9 parameters

Fit C: 7 parameters

B_g=C_g=0

Data selection:

Q^2> 5 GeV^2, ξ<0.1

375 data points

Q^2 cut chosen to avoid large higher twist contributions

Much smaller uncertainty for the quark diffractive PDF at high z

Diffractive PDFs from fits to 18 GeV x 275 GeV data

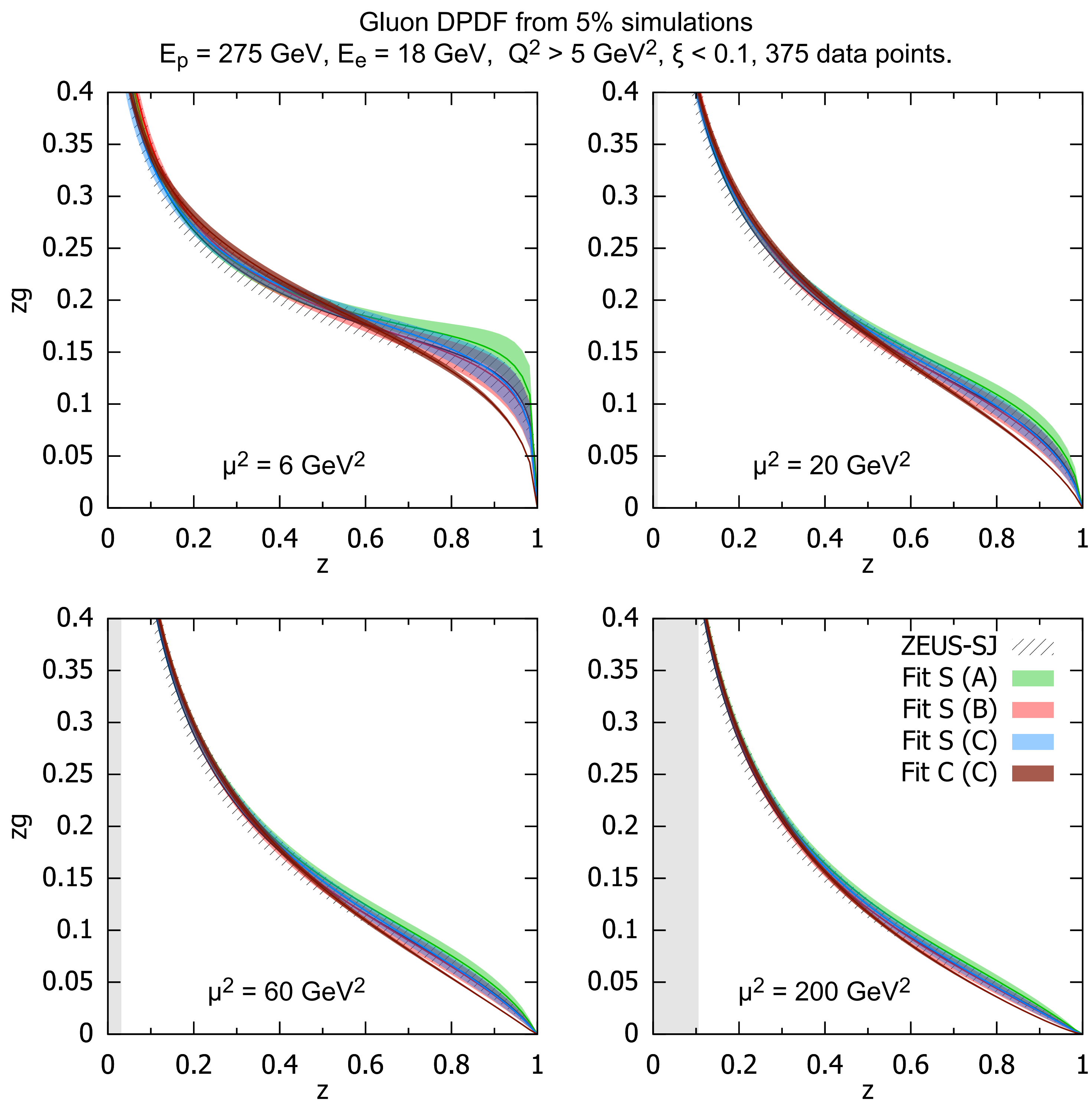

Gluon diffractive PDF

Fit S: 9 parameters

Fit C: 7 parameters

$B_g = C_g = 0$

Data selection:

$Q^2 > 5$ GeV^2, $\xi < 0.1$

375 data points

No improvement for the gluon density

Both fits C and S are comparable

Another process needed, dijet production to constrain the gluon at large z (like at HERA)

Perform study at lower systematics

Inclusive diffraction on nuclei

Nuclear shadowing and diffraction are related (Gribov)

Nuclear modification factors from the model by Frankfurt-Guzey-Strikman

High quality data

Two scenarios for high (H) and low (L) shadowing considered

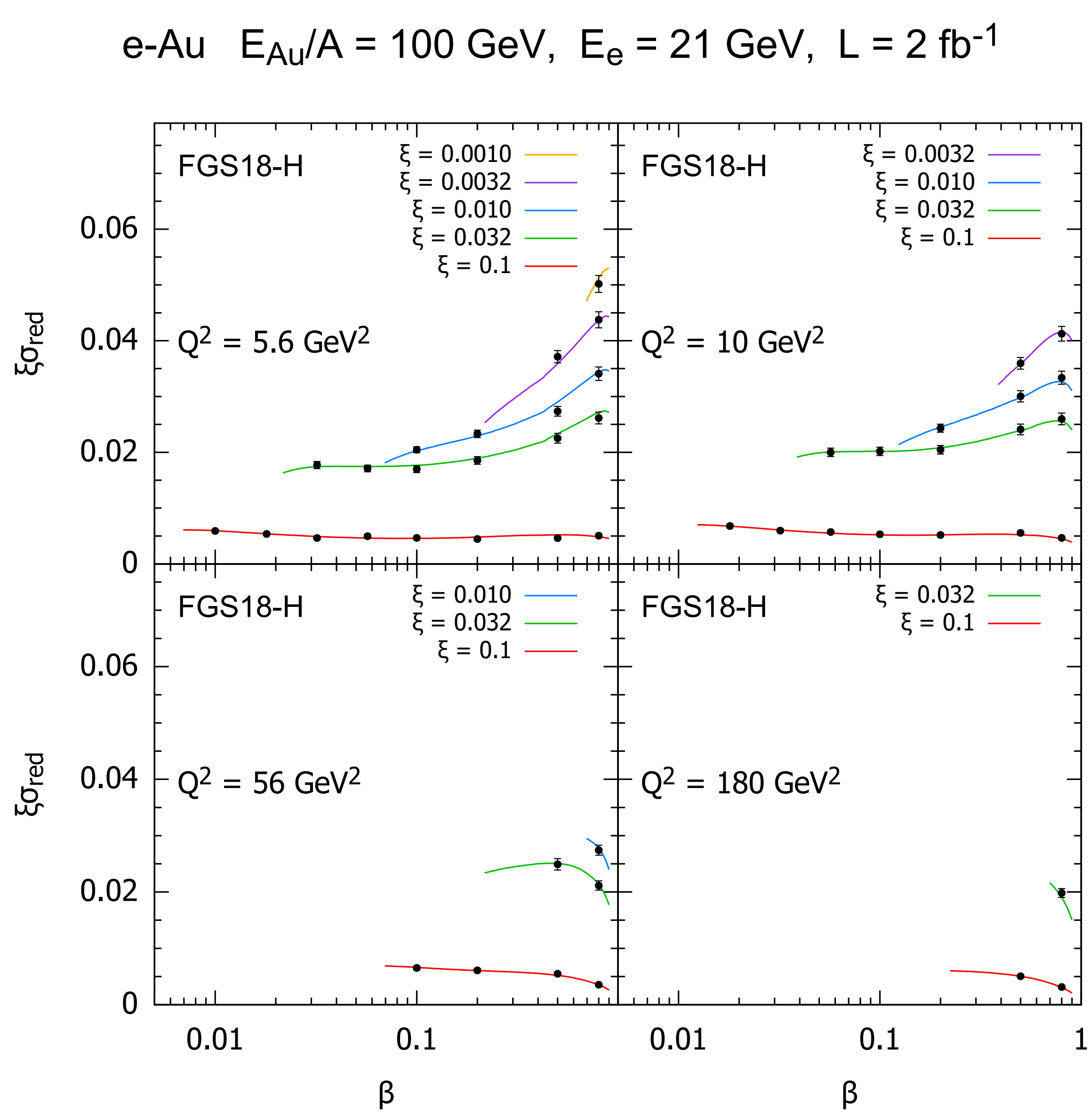

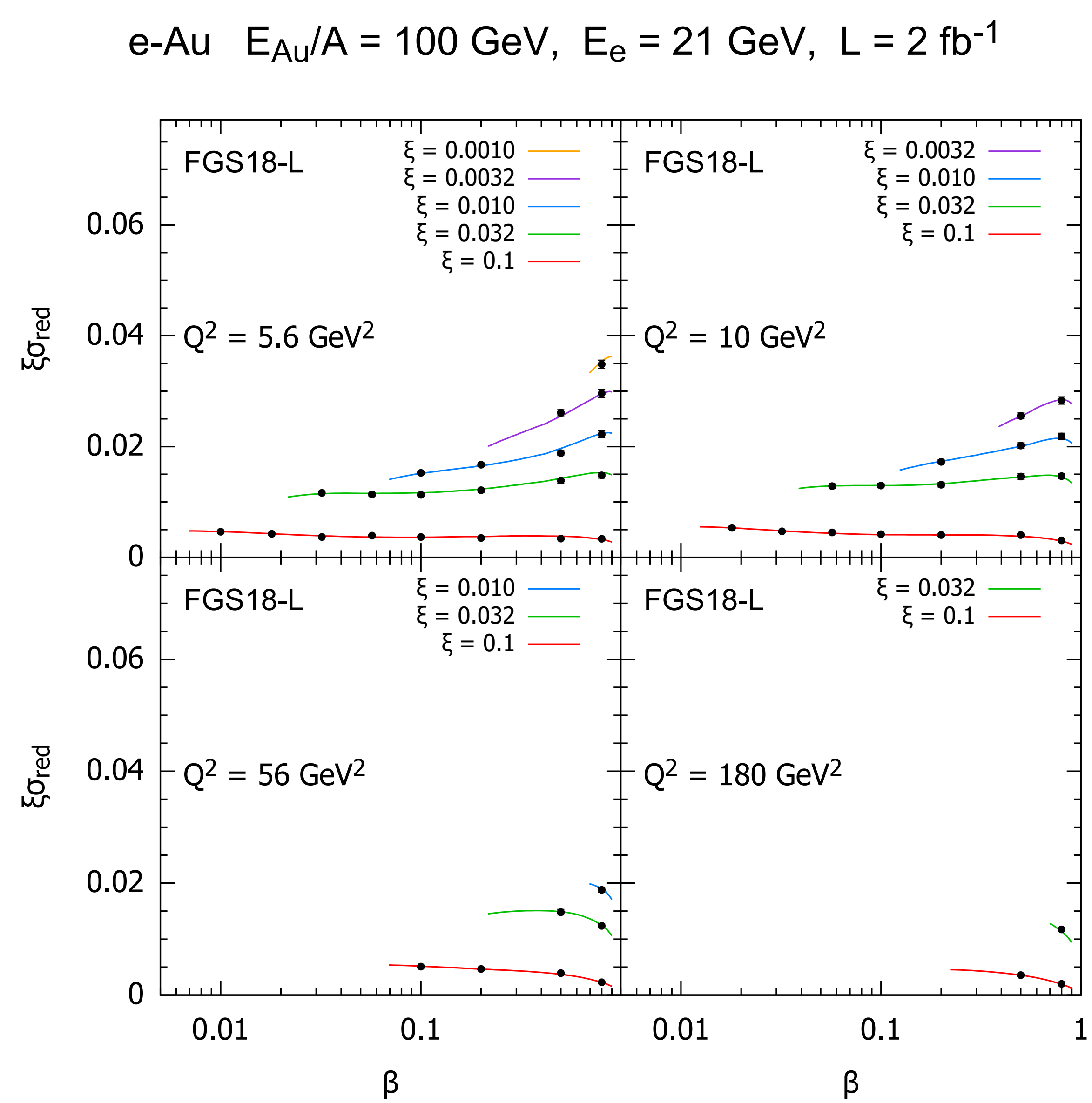

Pomeron, Reggeon and F_2, F_L component to $\sigma^{D(3)}$

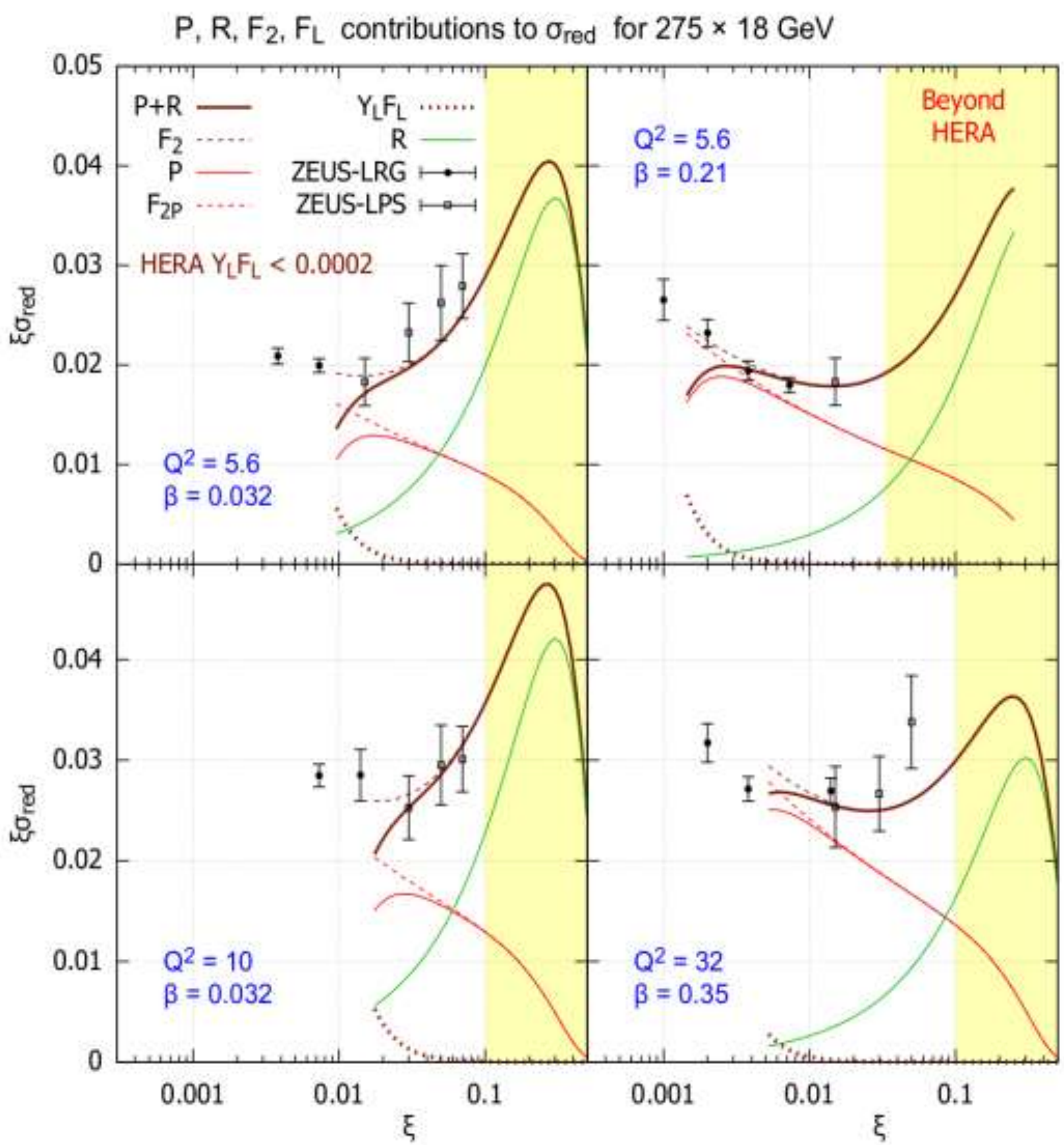

Pomeron dominates at low ξ

Reggeon dominates at high ξ>0.05

High ξ region accessible by the final proton tagging at the EIC

$$\sigma^{\mathrm{D}}_{\mathrm{red}} = F^{\mathrm{D}}_2 - \frac{y^2}{1+(1-y)^2} F^{\mathrm{D}}_L$$

Significant F_L component, about 30 times larger than at HERA due to higher y values

$$y = \frac{Q^2}{xs} = \frac{Q^2}{\beta \xi s}$$

Why $F_L^{D(3)}$ is interesting? $F_L^{D(3)}$ at HERA

Why F_L^D is interesting?

F_L^D vanishes in the parton model

Gets non-vanishing contributions in QCD

As in inclusive case, particularly sensitive to the diffractive **gluon density**

Expected large **higher twists**, provides test of the **non-linear, saturation** phenomena

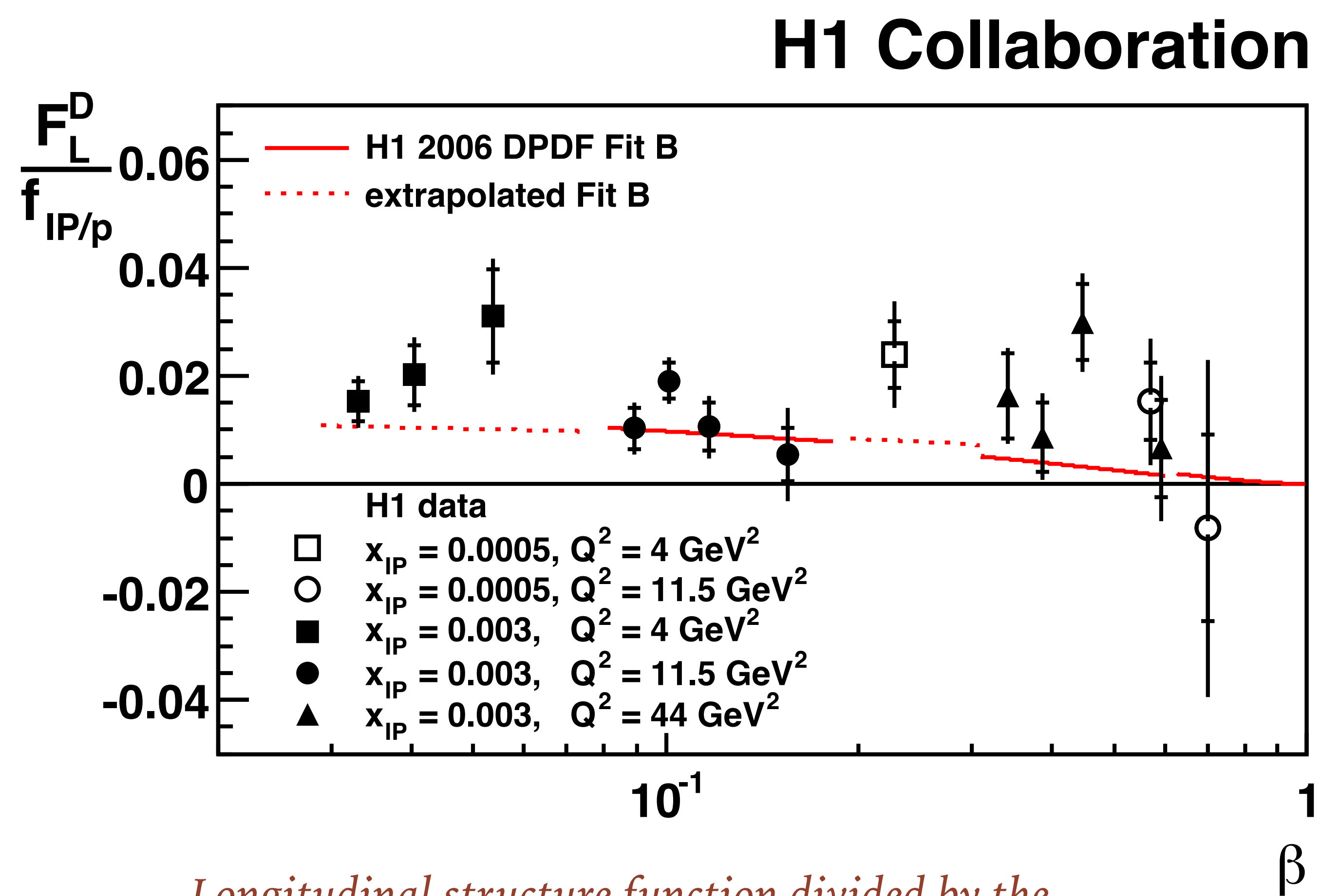

Longitudinal structure function divided by the reduced cross section

Experimentally challenging…

Measurement requires several beam energies

H1 measurement: 4 energies, E_p=920, 820, 575, 460 GeV, electron beam E_e=27.6 GeV

Large errors, limited by statistics at HERA

Careful evaluation of systematics. Best precision 4%, with uncorrelated sources as low as 2%

Pseudodata generation for F_L: energy choice

$$\sigma_{\rm red}^{\rm D(3)} = F_2^{\rm D(3)}(\beta,\xi,Q^2) - Y_{\rm L}\, F_{\rm L}^{\rm D(3)}(\beta,\xi,Q^2)$$

Integrated over t-momentum transfer

$$Y_{\rm L} = \frac{y^2}{Y_+} = \frac{y^2}{1+(1-y)^2}$$

Can disentangle $F_2^{D(3)}$ from $F_L^{D(3)}$ by varying energy and performing the linear fit.

$$y = \frac{Q^2}{xs} = \frac{Q^2}{\beta\xi s}$$

Need to vary the energy $\sqrt{s}$ to change y for fixed (β,ξ,Q^2)

EIC energies for electron and proton:

$$E_e = 5{,}10{,}18 \text{ GeV}$$

$$E_p = 41{,}100{,}120{,}165{,}180{,}275 \text{ GeV}$$

	E_p [GeV] 41	100	120	165	180	275
E_e [GeV] 5	**29**	**45**	49	**57**	60	74
10	40	**63**	69	**81**	85	**105**
18	54	**85**	93	**109**	114	**141**

S-17 all 17 combinations

S-9 9 - bold red

S-5 5 - green (EIC preferred)

Pseudodata generation

Binning and cuts

Uniform logarithmic binning, 4 bins per order of magnitude in each β, Q^2, ξ

Bins in (ξ, β, Q^2), common to at least four beam setups

$Q^2 > 3$ GeV^2 both H1 and ZEUS fits indicate deterioration of fits for low Q^2

$0.96 > y > 0.005$ expected coverage of the experiment

Simulations

Cross section generation from ZEUS-SJ diffractive PDFs evolved with DGLAP

Assumed δ_{sys}=1-2%, extrapolated from HERA 2% uncorrelated systematics; normalization/correlated systematics negligible effect on extraction of F_L^D

δ_{stat} from 10 fb^{-1} integrated luminosity

Several random samples are generated

Kinematic range and number of points

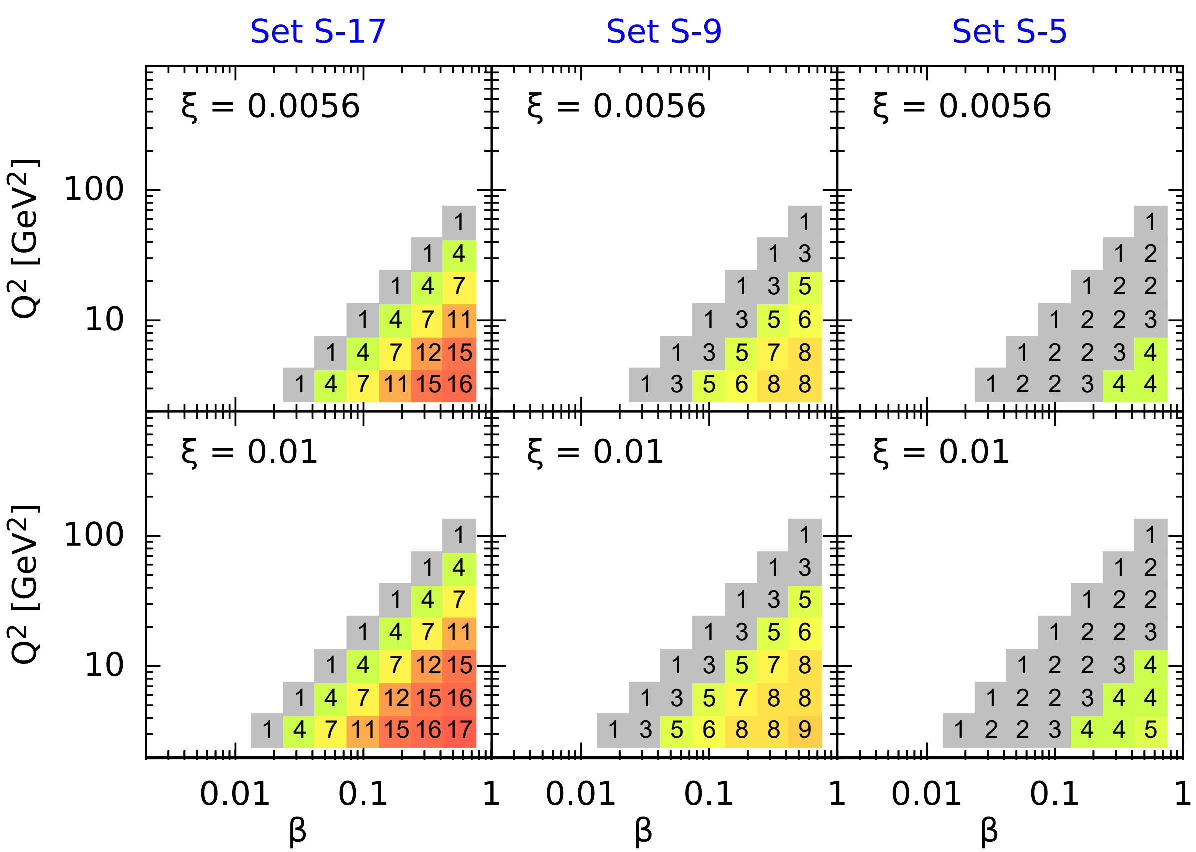

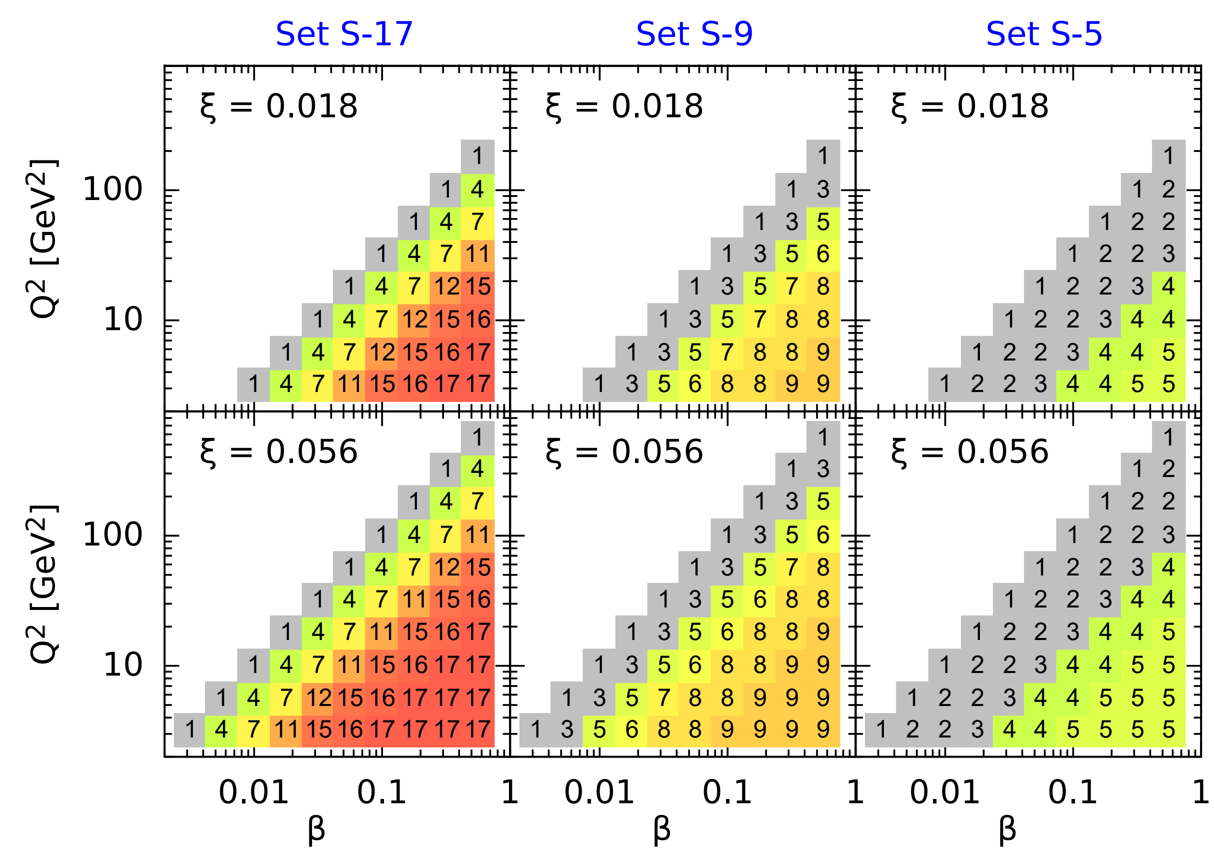

Count of different beam energy combinations for S-17, S-9, S-5

Only points with more than 4 combinations are taken for F_L extraction

Set-17: 364, set-9: 285, set-5: 160 values of F_L

$F_L^{D(3)}$ extraction

$\sigma_r = F_2(\xi, \beta, Q^2) - Y_L F_L(\xi, \beta, Q^2)$ as a function of Y_L

Bins in (ξ, β, Q^2)

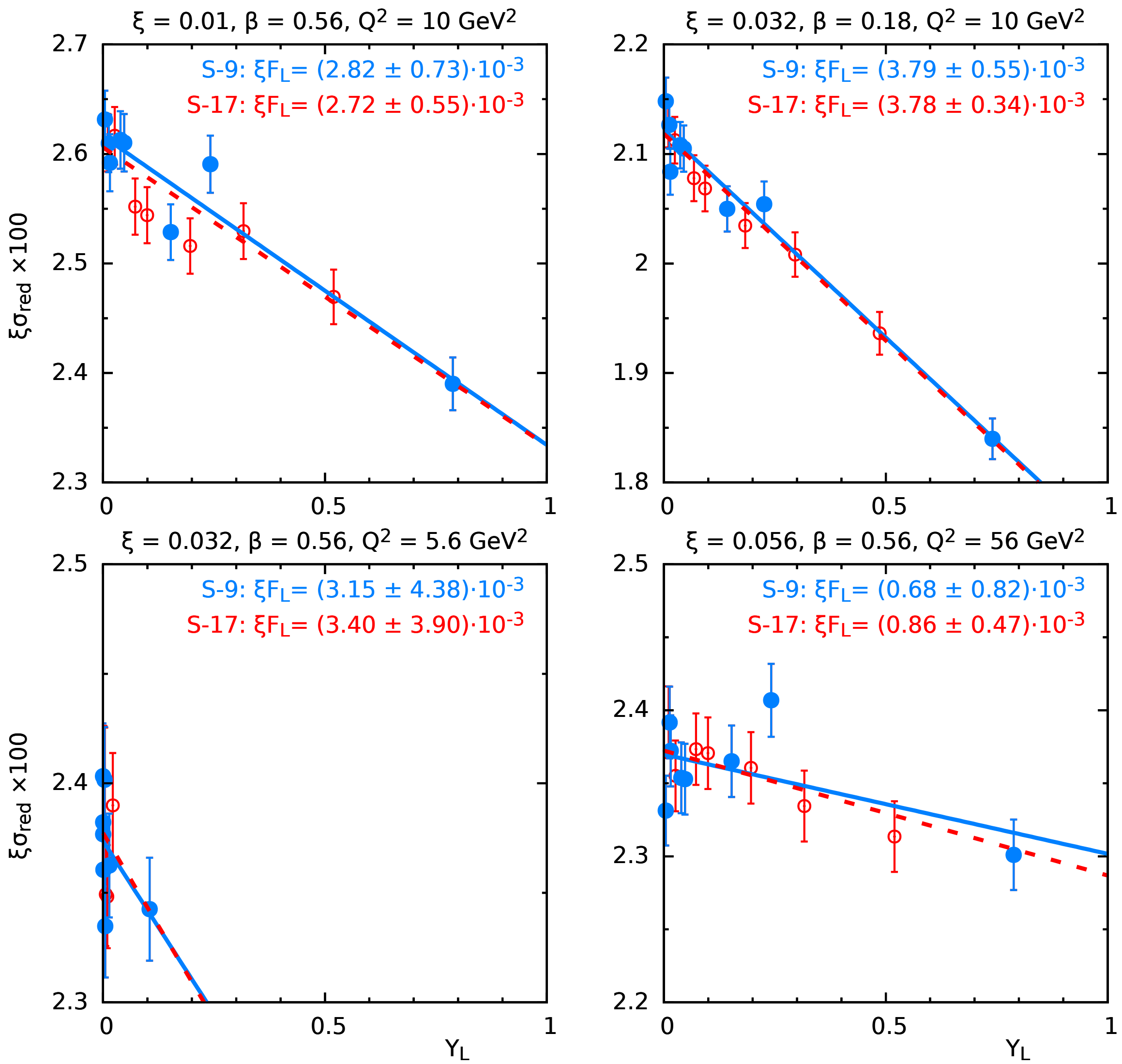

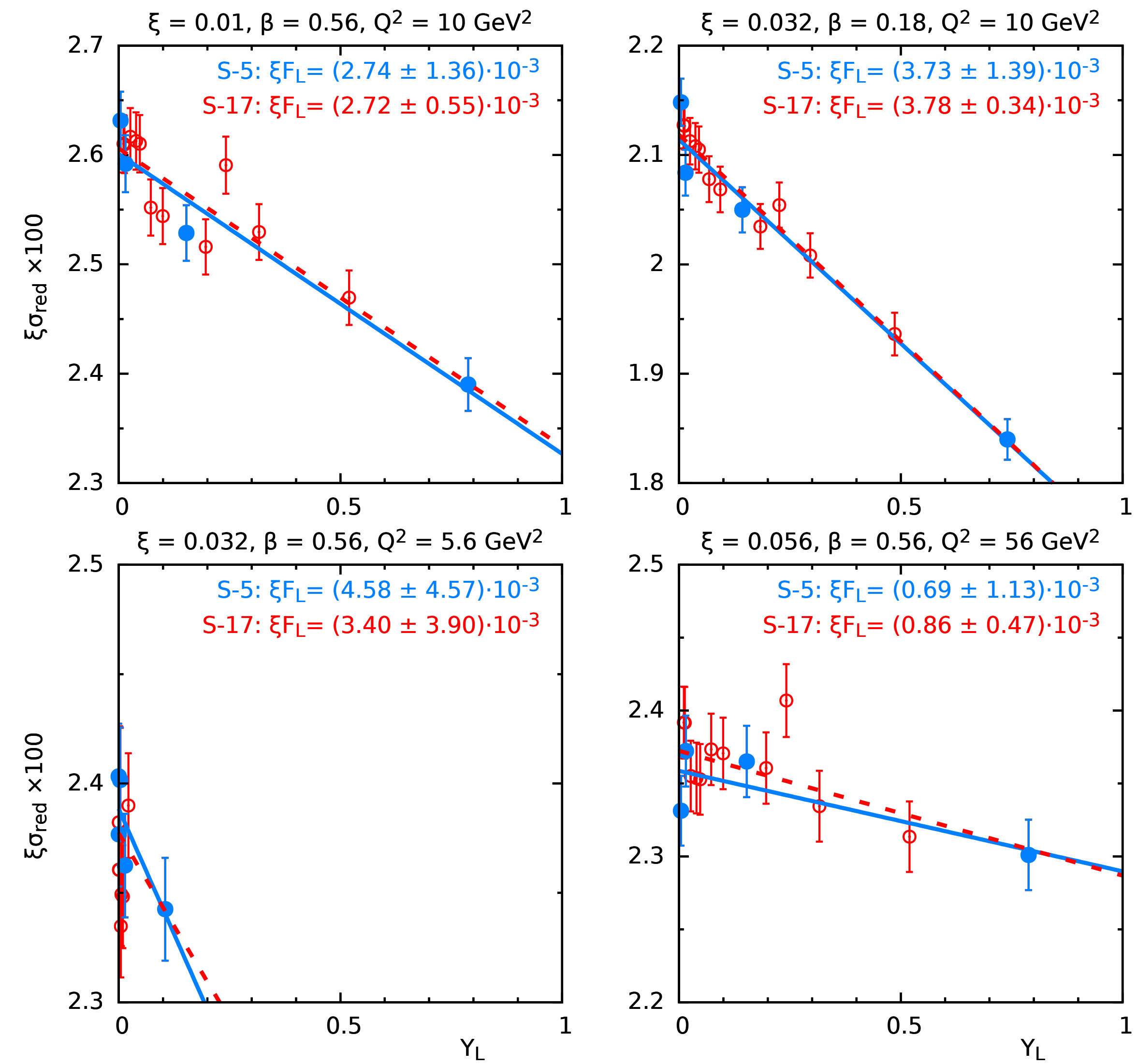

Uncorrelated systematics 1%

Differences between S-17 and S-9, S-5 small

Increase in error bar on the extraction when smaller number of energy points

Largest errors for bins with shortest range of Y_L

Simulated measurement of $F_L^{D(3)}$ vs β in bins of (ξ, Q^2)

Systematic error 1%, 5 MC samples to illustrate fluctuations

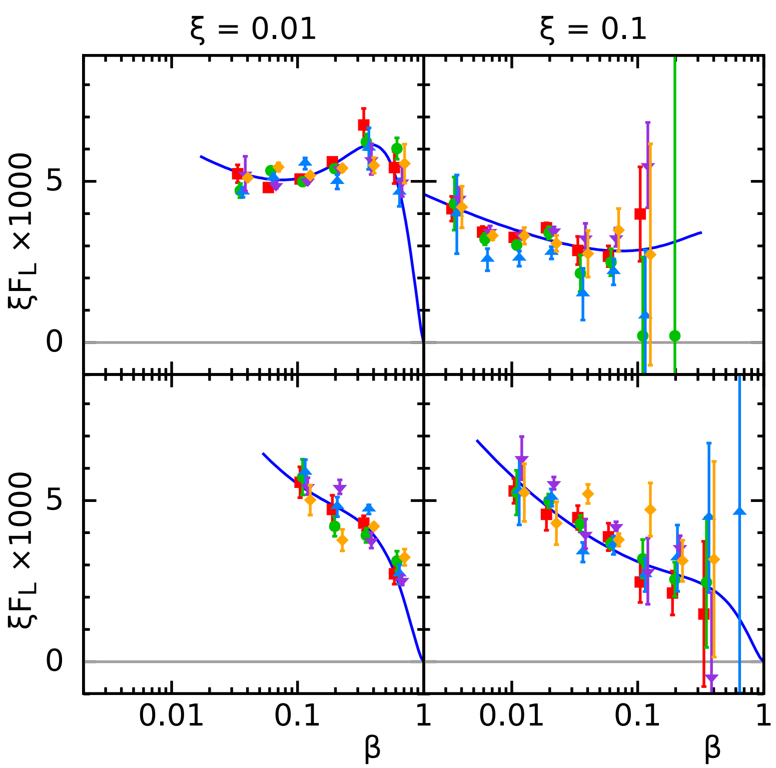

17 energies

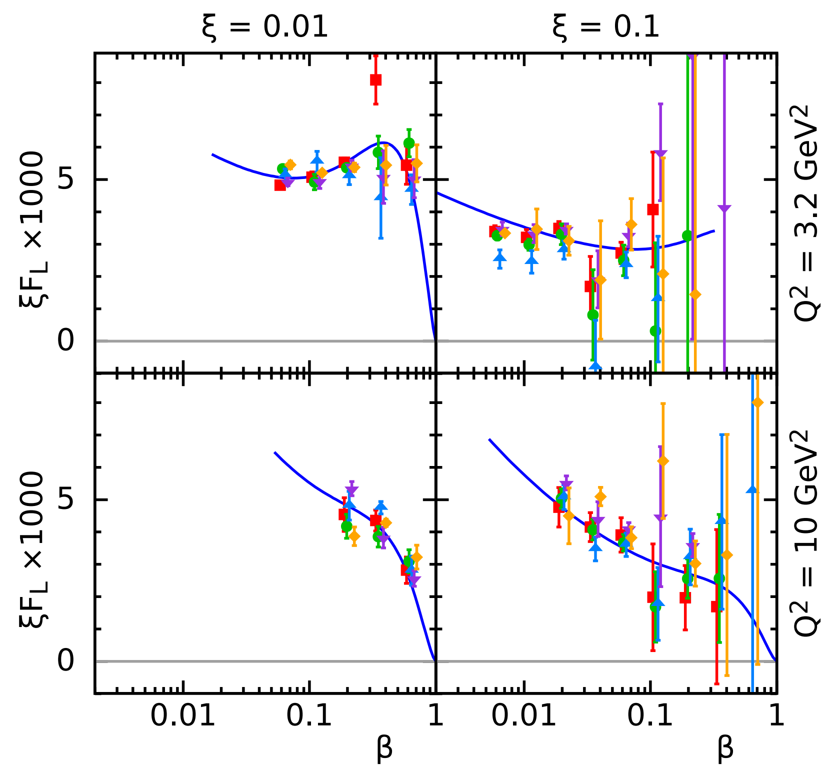

9 energies

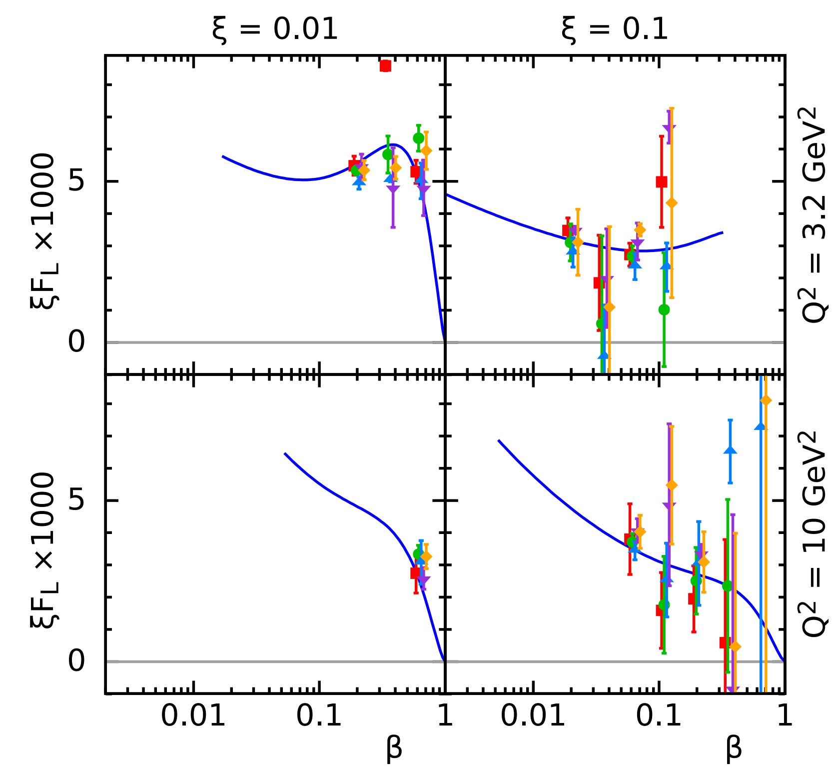

5 energies

Small differences between S-17 and S-9, small reduction to range and increase in uncertainties.

More pronounced reduction in range and higher uncertainties in S-5.

An extraction of F^D_L possible with EIC-favored set of energy combinations

Simulated measurement of $F_L^{D(3)}$ vs β in bins of (ξ,Q^2)

S-17

$\delta_{\text{sys}} = 1\,\%$

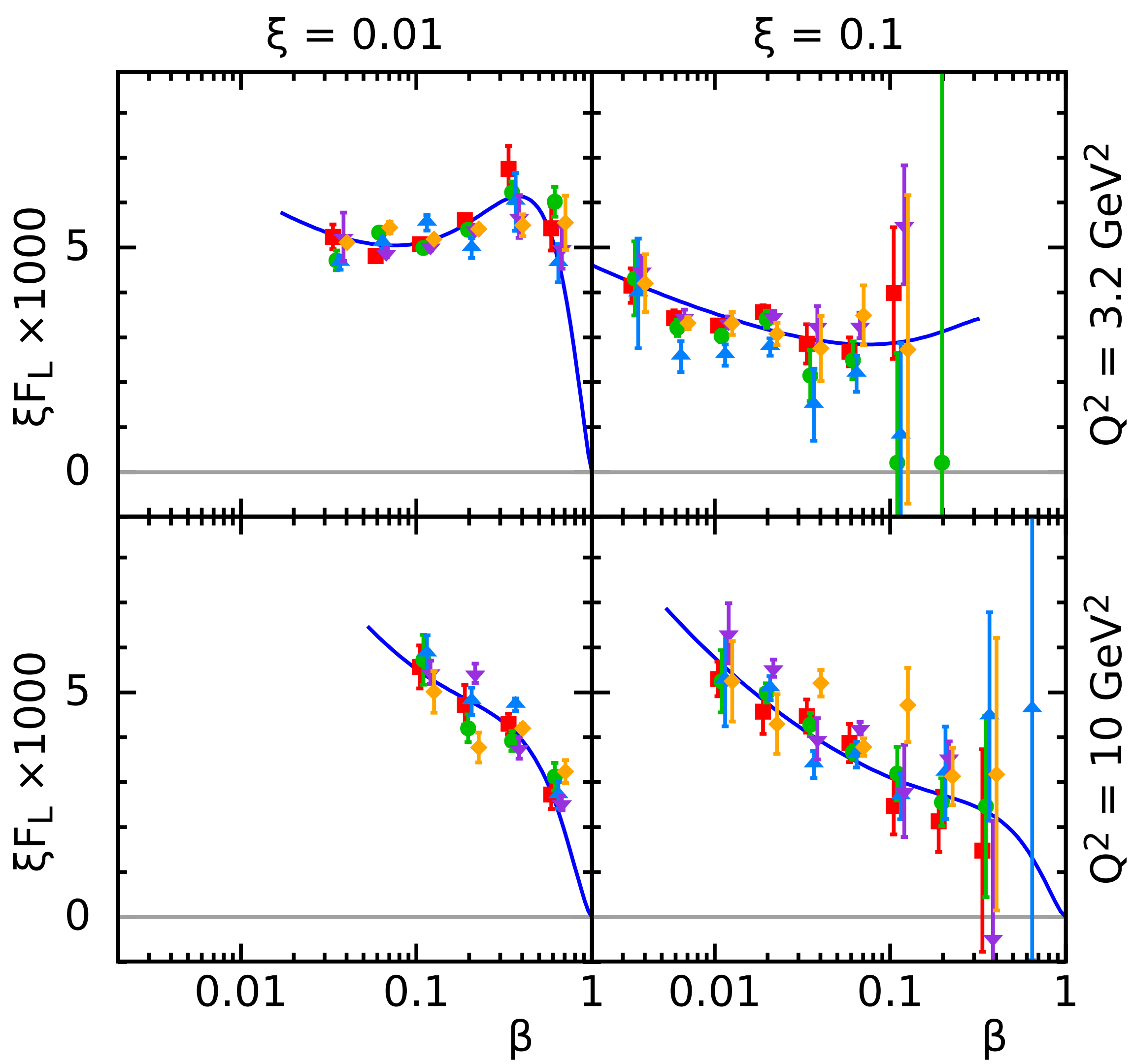

$\delta_{\text{sys}} = 2\,\%$

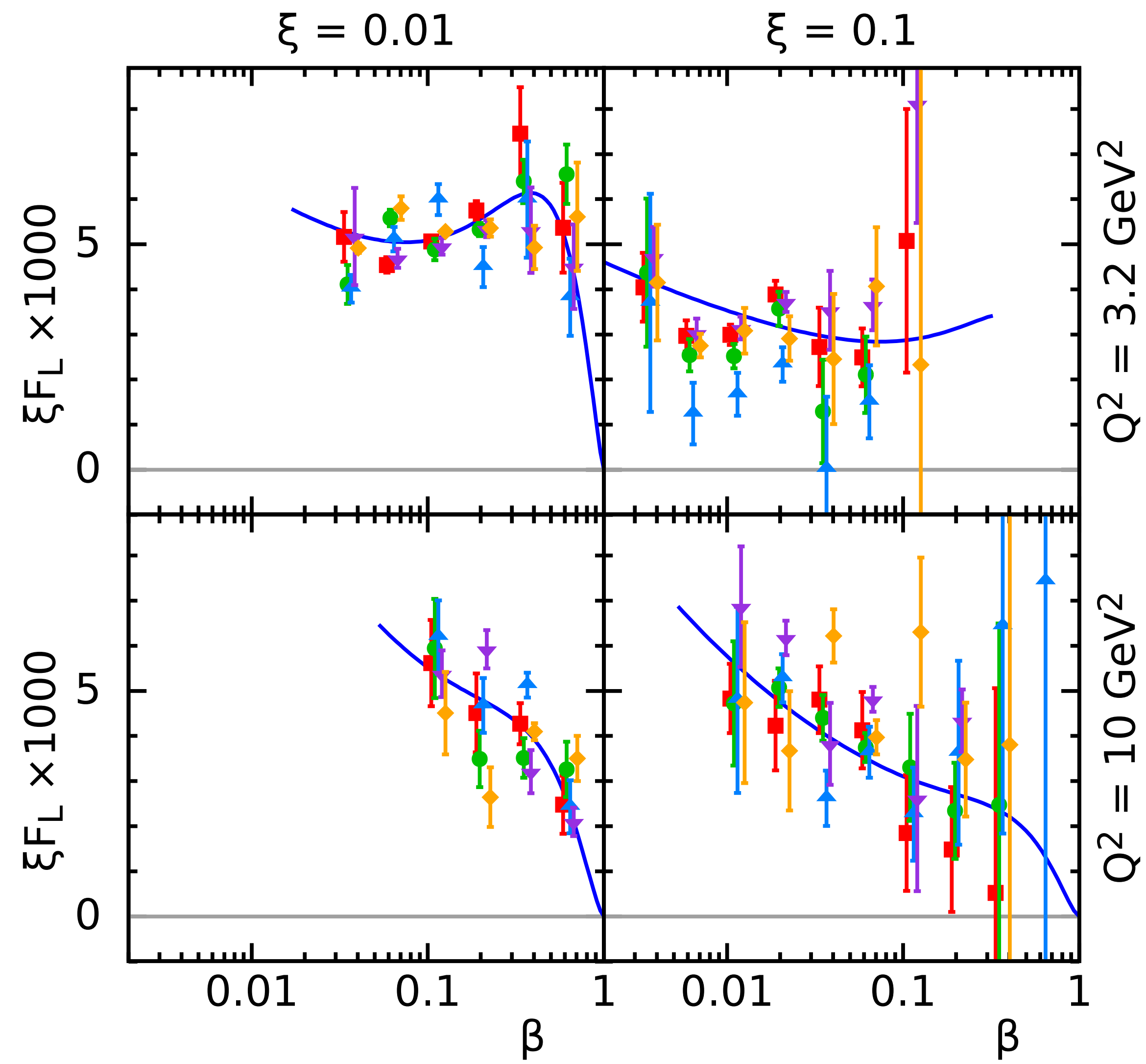

Change from 1% to 2% results in roughly twice large error bars

Statistical errors negligible

$F_L^{D(3)}$ fit accuracy

Estimate the accuracy of extraction for $F_L^{D(3)}$

Generate several MC samples of pseudodata and perform fits

Use direct arithmetic averaging neglecting the uncertainties from the fits

average

$$\bar{v} = \frac{S_1}{N}$$

$$S_n = \sum_{i=1}^{N} v_i^n$$

variance

$$(\Delta v)^2 = \frac{S_2 - S_1^2/N}{N-1}$$

Where v_i is the value of F_L^D in Monte Carlo sample i

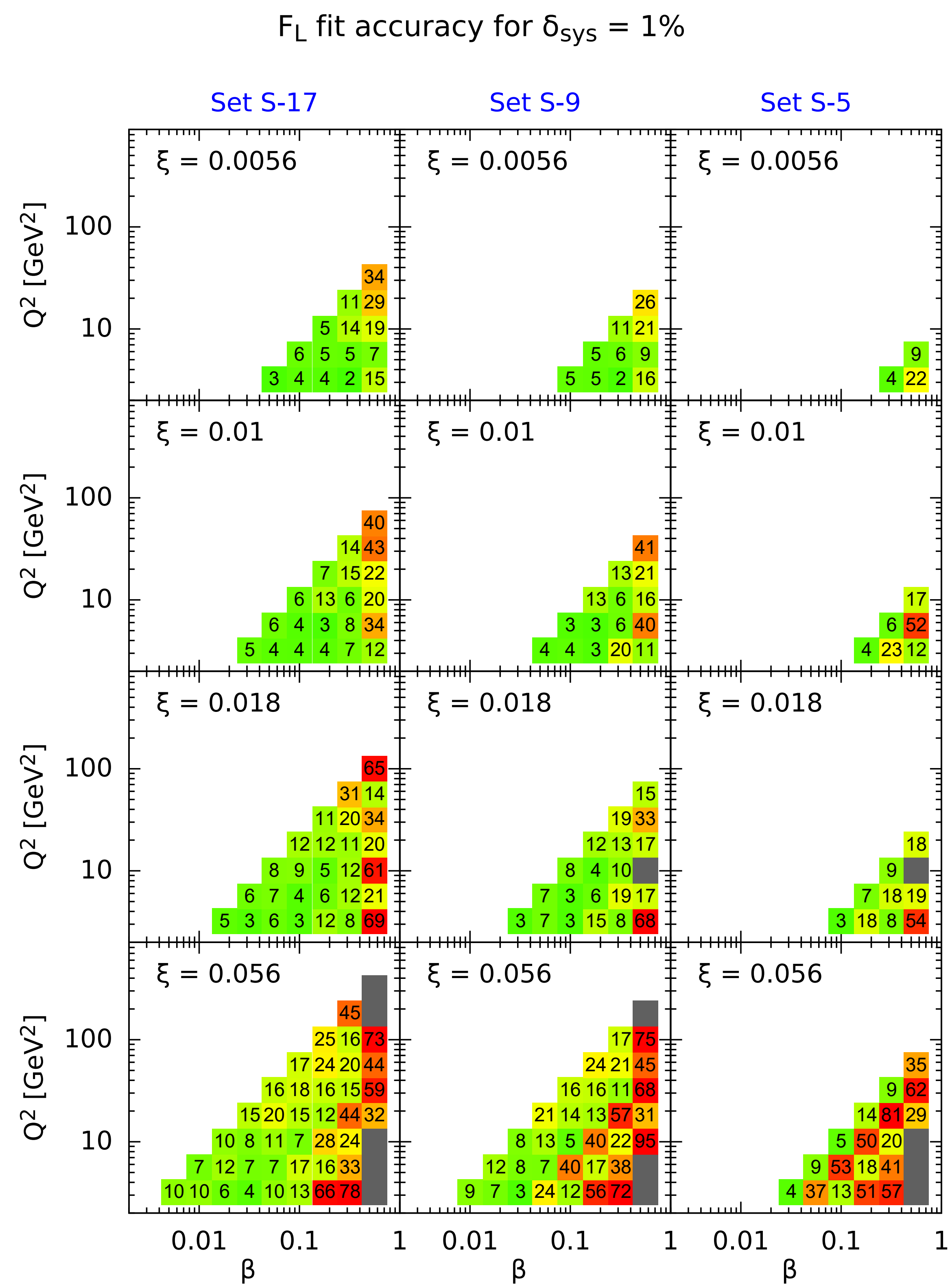

$R^D = F_L^D / F_T^D$ ratio of longitudinal to transverse

Ratio of cross section for longitudinally polarized photons to cross sections for transverse polarized photons

$$R^{D(3)} = F_L^{D(3)} / F_T^{D(3)}$$

$$F_T^{D(3)} = F_2^{D(3)} - F_L^{D(3)}$$

$$\sigma_{\rm red}^{D(3)} = [1 + (1 - Y_L) R^{D(3)}] F_T^{D(3)}$$

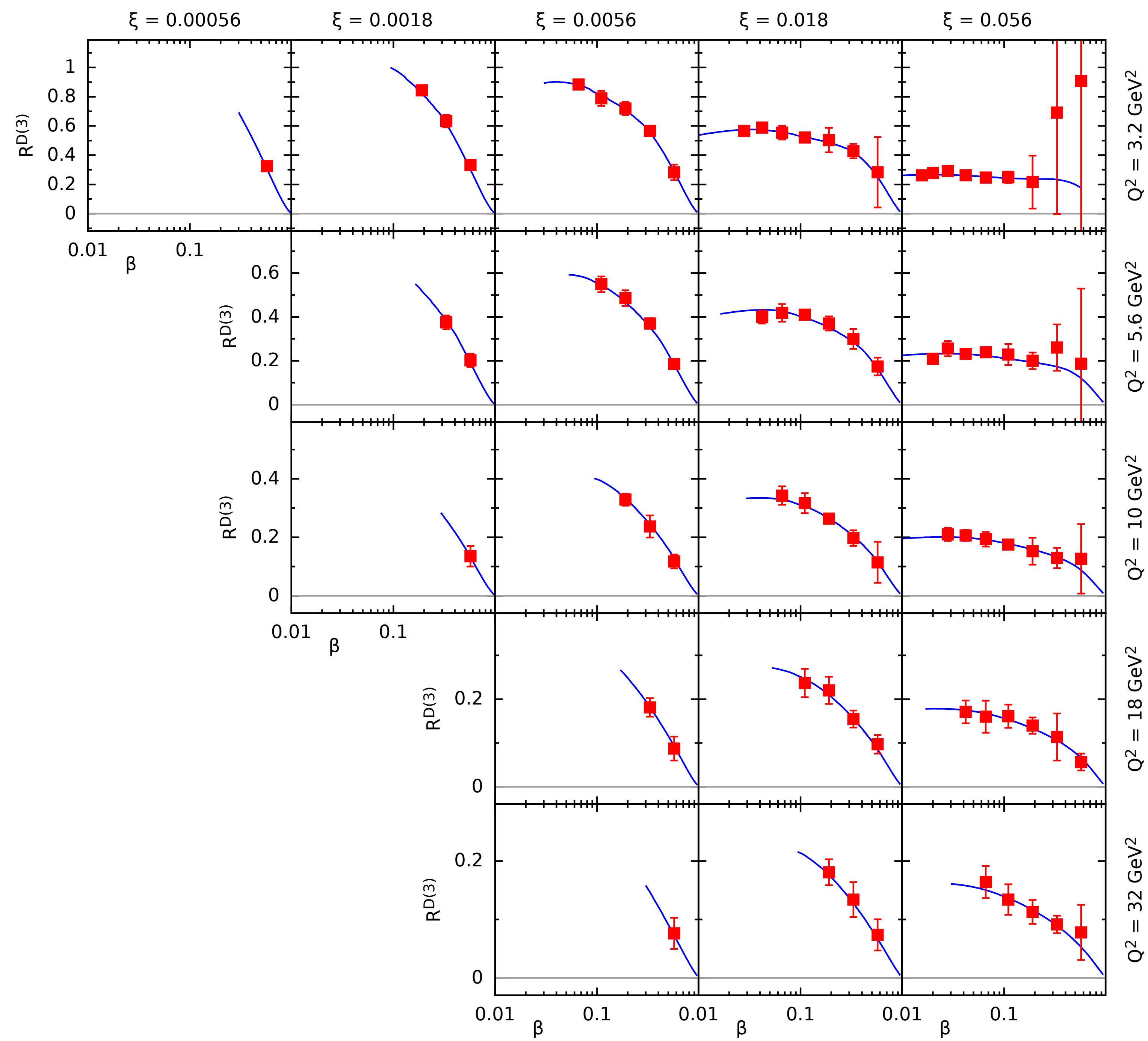

Different form of reduced cross section

Alternative fit has different sensitivities to the uncertainties

Systematics 1%

Averaged over 10 MC samples: reduced fluctuations

Simulations of $\sigma^{D(4)}$

High luminosity and excellent possibility of proton tagging

Prospect of high quality data for $\sigma_{\mathrm{r}}^{D(4)}(\xi, \beta, Q^2, t)$

From the ZEUS-SJ fit

$$\xi \varphi_P(\xi, t) \propto \xi^{-0.22}\, e^{-7|t|}$$

$$\xi \varphi_R(\xi, t) \propto \xi^{0.6+1.8|t|}\, e^{-2|t|}$$

Very different slopes in t for Reggeon and Pomeron

Extrapolation of reduced cross section using ZEUS SJ fit

Random smearing with errors:

Systematic: $\delta_{sys} = 5\ \%$

Statistics: δ_{stat} from integrated luminosity 10 fb^{-1}

$\sigma^{D(4)}$ vs t

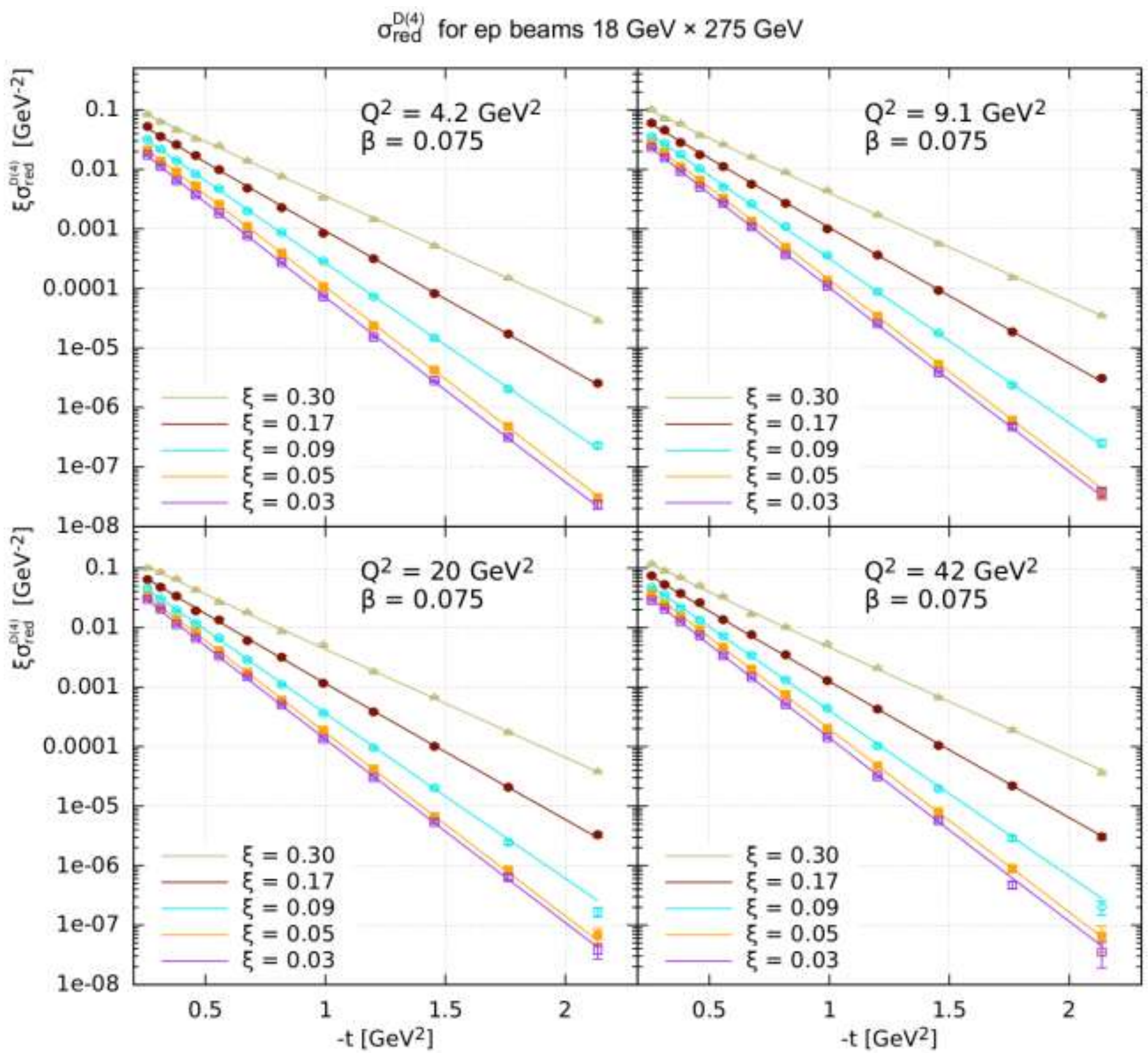

$E_e = 18$ GeV
$E_p = 275$ GeV

Lines — extrapolation
Points — simulation

Very well measurable
t-slope vs. ξ

DIS2021 - Wojtek Słomiński - Jagiellonian University 16

$\sigma^{D(4)}$ vs ξ

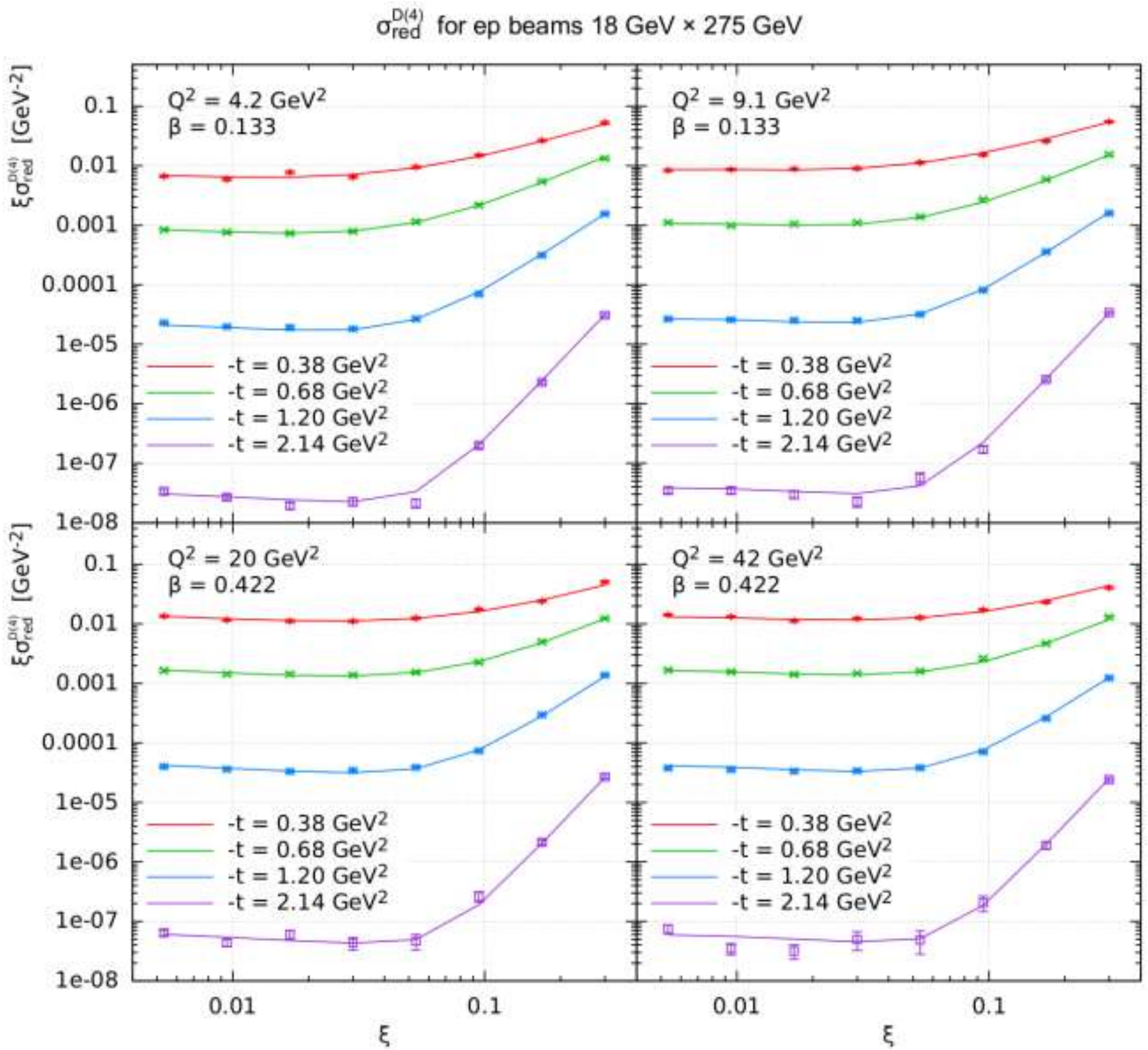

$E_e = 18$ GeV
$E_p = 275$ GeV

Lines — extrapolation
Points — simulation

Very well measurable dependence on ξ

Double-slope structure?

DIS2021 - Wojtek Słomiński - Jagiellonian University 17

Diffractive elastic vector meson production

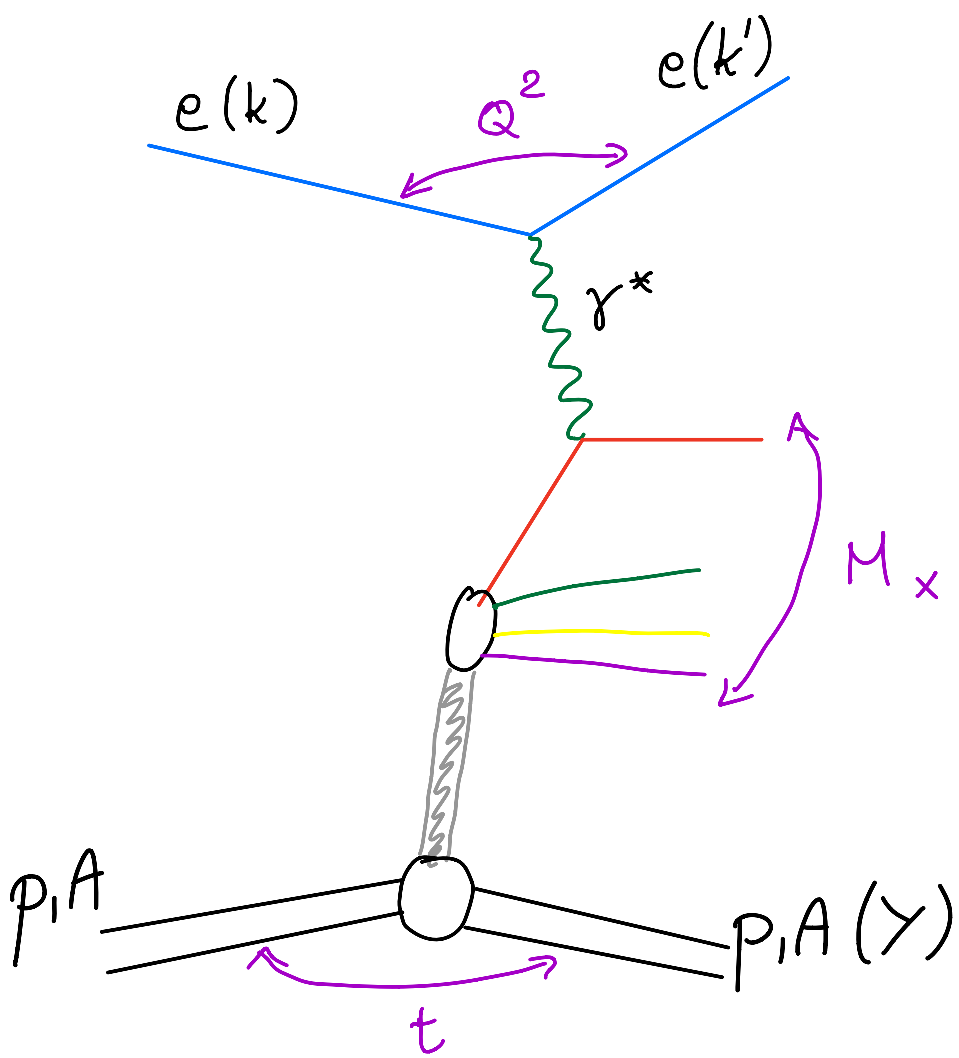

Final state contains only vector meson, scattered lepton and proton

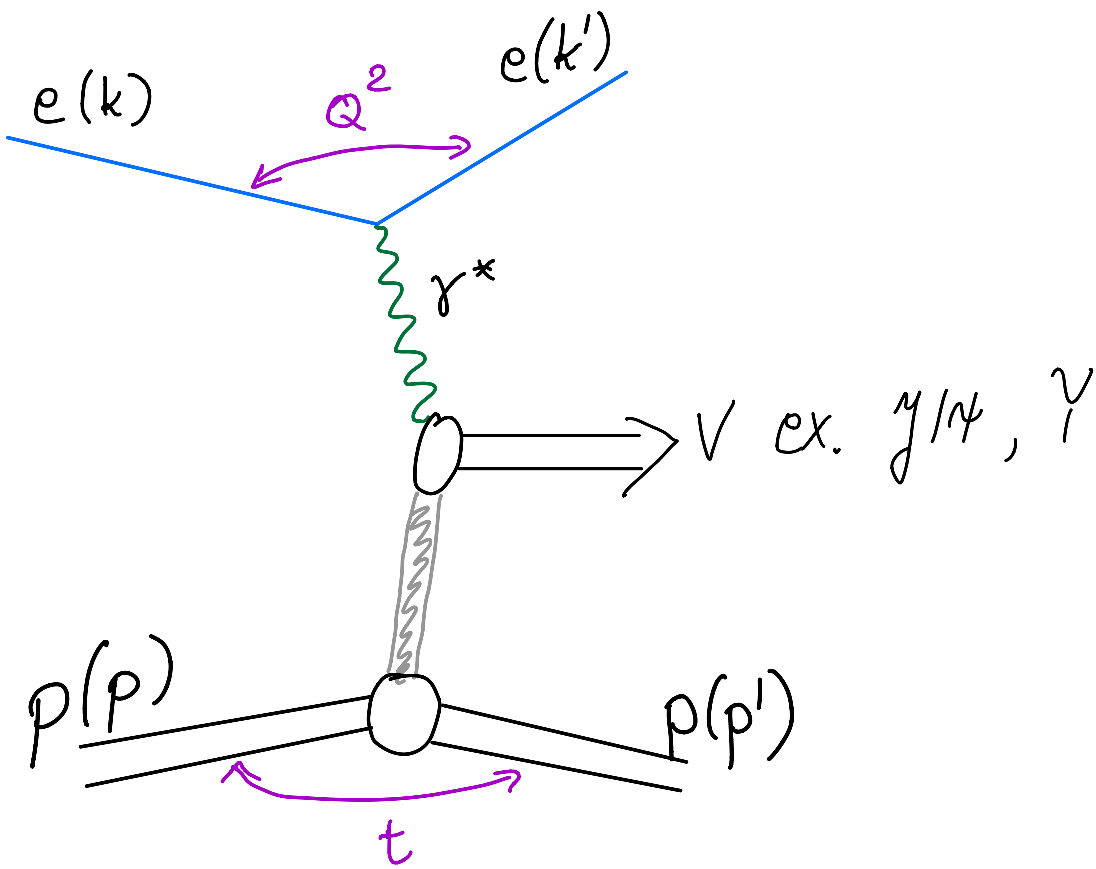

J/ψ vector meson: charm -anti charm system $m = 3.09 \text{ GeV}$

Upsilon vector meson: bottom - anti bottom system $m = 9.46 \text{ GeV}$

Elastic vector meson production

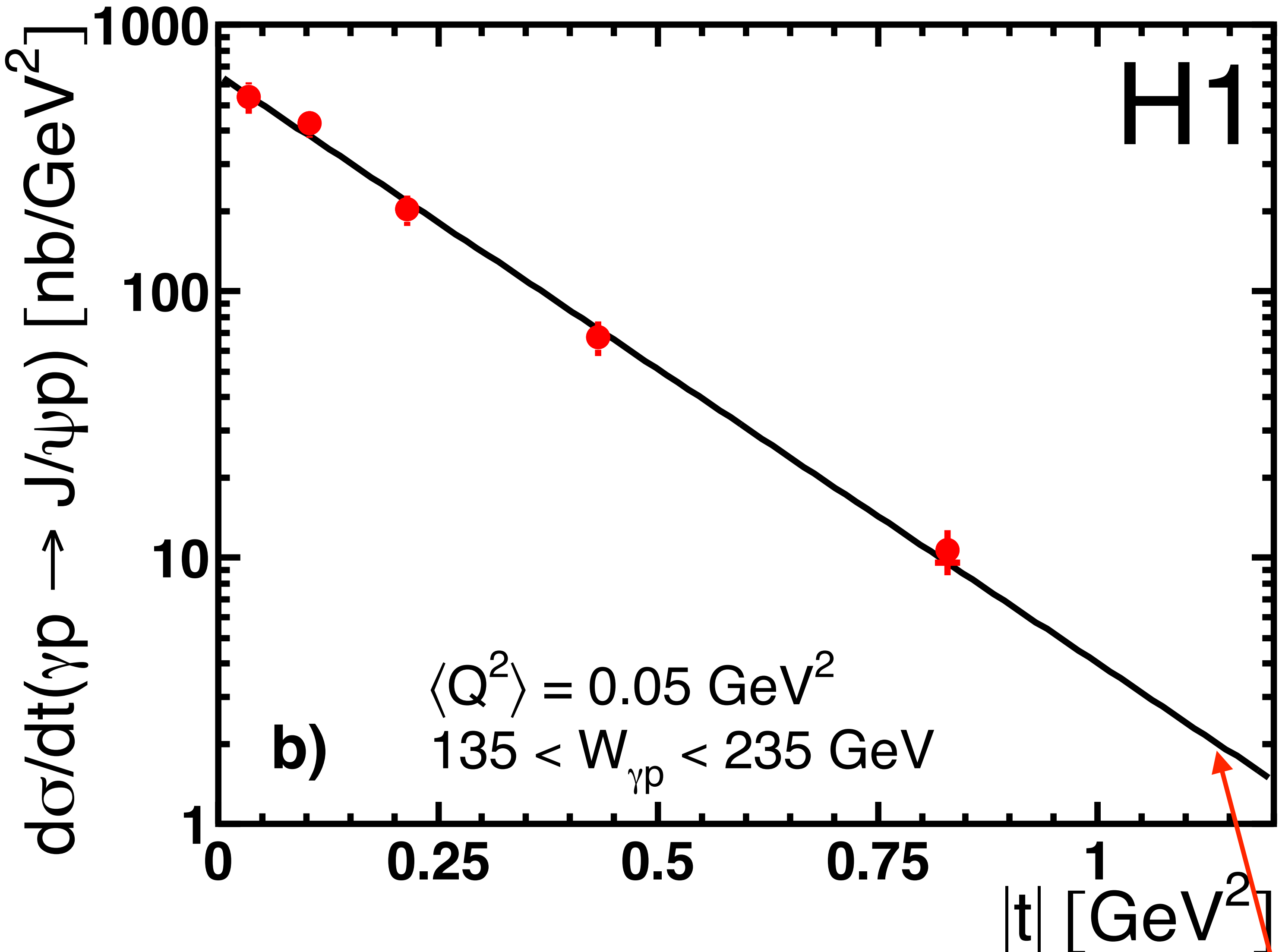

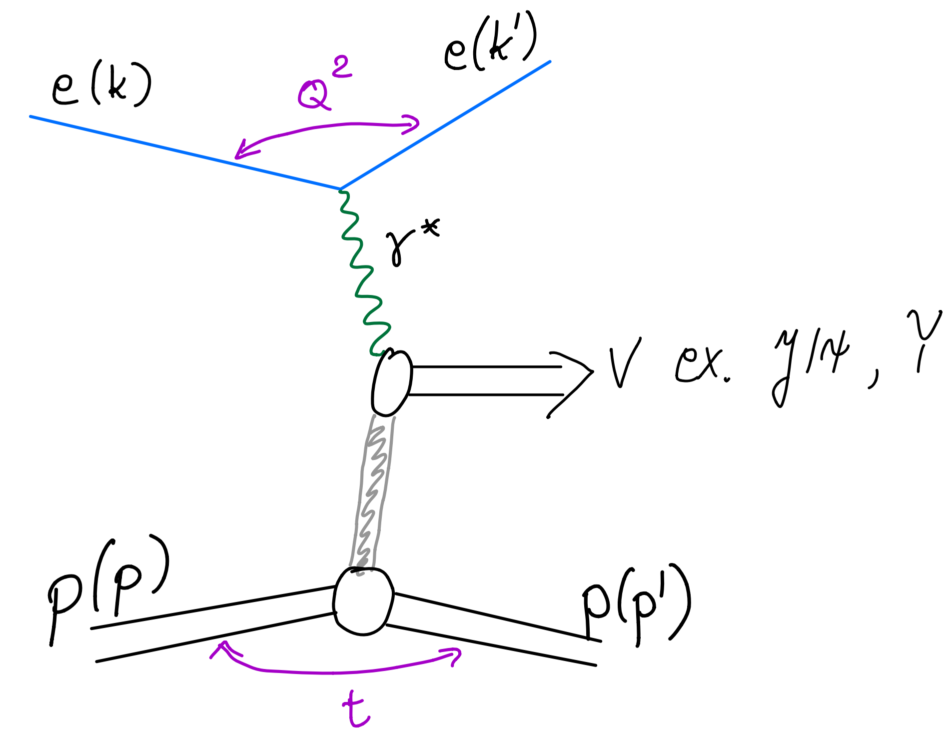

$$t = (p - p')^2 < 0$$

momentum transfer at the proton vertex

$$\frac{d\sigma}{dt} \sim e^{bt}$$

Exponential fit

Extraction of density profile in impact parameter

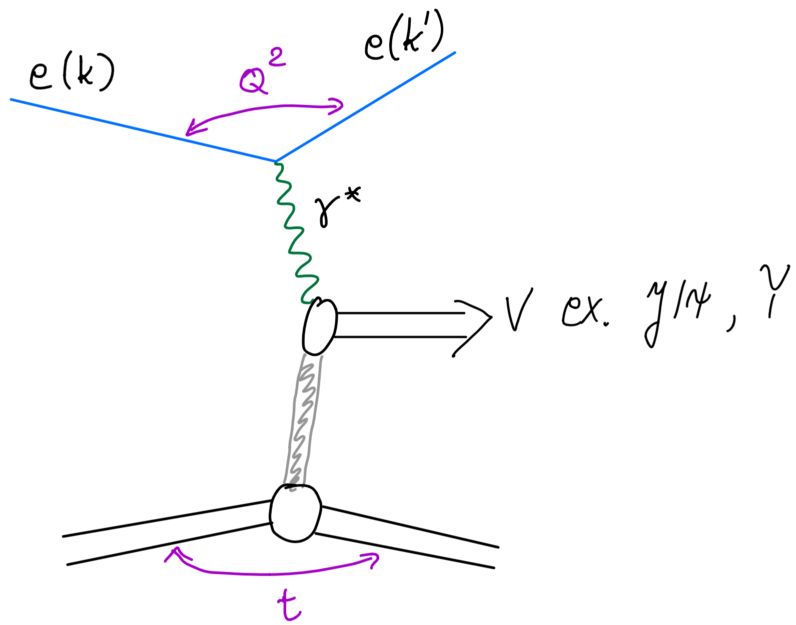

Momentum transfer $t = -\Delta^2$

$$\frac{d\sigma}{dt} = \frac{1}{16\pi}|\mathcal{M}(\Delta)|^2$$

$$\mathcal{M}(\Delta) = \langle \psi_{\gamma^*} | A(\Delta) | \psi_V \rangle$$

$\mathcal{M}$ amplitude for vector meson process

A elementary (quark dipole) amplitude

$$A(\Delta) = \int d^2\mathbf{b}\, e^{i\Delta\cdot\mathbf{b}} \tilde{A}(b)$$

$$\langle \tilde{A}(b) \rangle = \frac{\langle \psi_{\gamma^*} | \tilde{A} | \psi_V \rangle}{\langle \psi_{\gamma^*} | \psi_V \rangle} = \frac{\int d^2\Delta e^{-i\Delta b}\sqrt{\frac{d\sigma}{dt}}}{\pi^{3/2}\langle \psi_{\gamma^*} | \psi_V \rangle}$$

t-dependence of the elastic cross section provides information about the profile of the target

Diffractive elastic VM production

Diffractive elastic vector meson production as a way to study nucleon structure

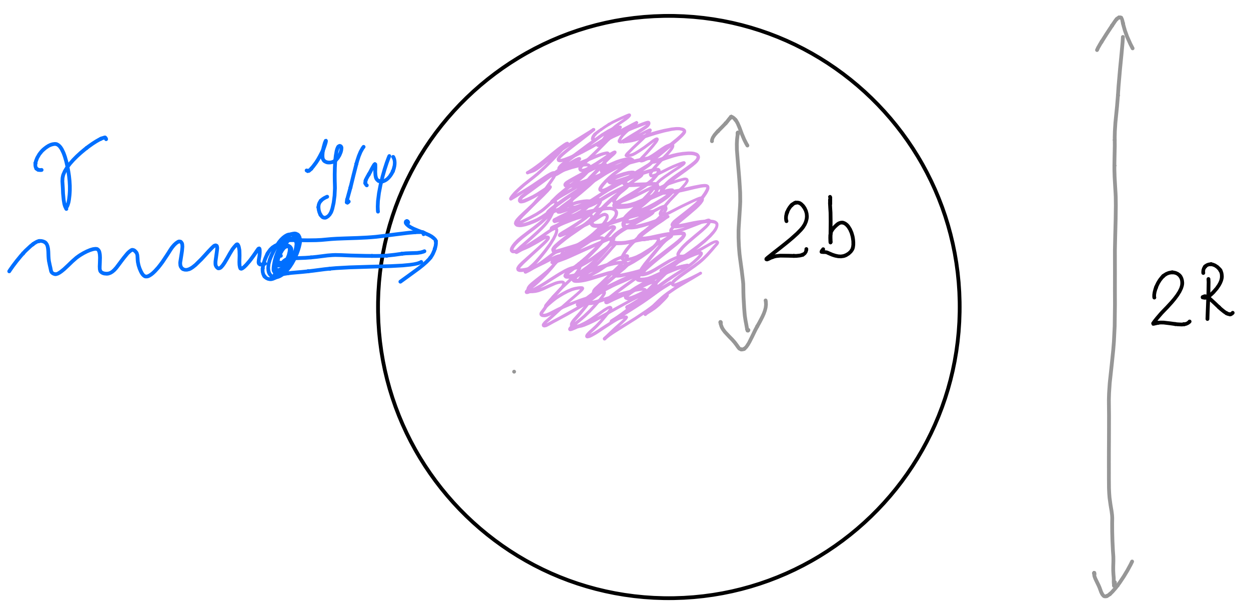

Radius measured in diffractive scattering of vector mesons

$$b \approx 0.5 \div 0.6 \text{ fm}$$

Proton charge radius

$$R \approx 0.84 \div 0.87 \text{ fm}$$

Experiments on elastic VM production suggest gluons are concentrated in smaller regions than quarks

Growth of the target size with energy

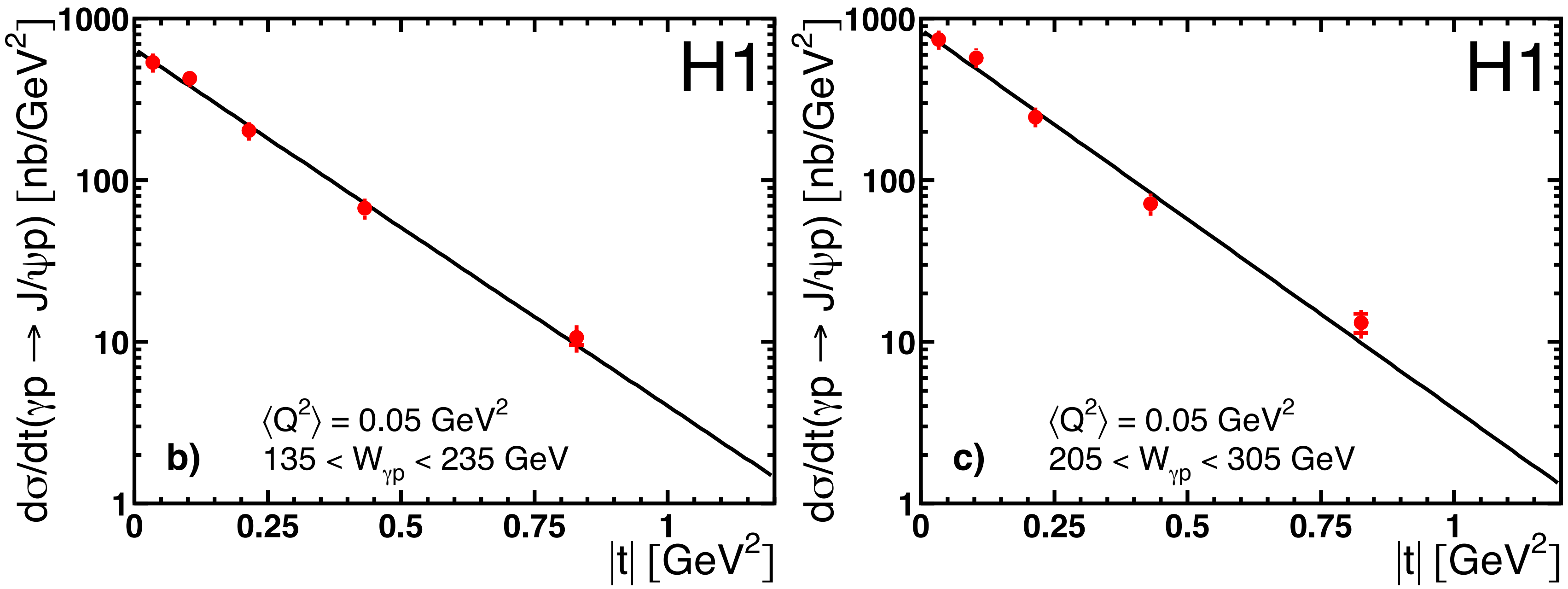

$$\frac{d\sigma}{dt} \sim e^{bt}$$

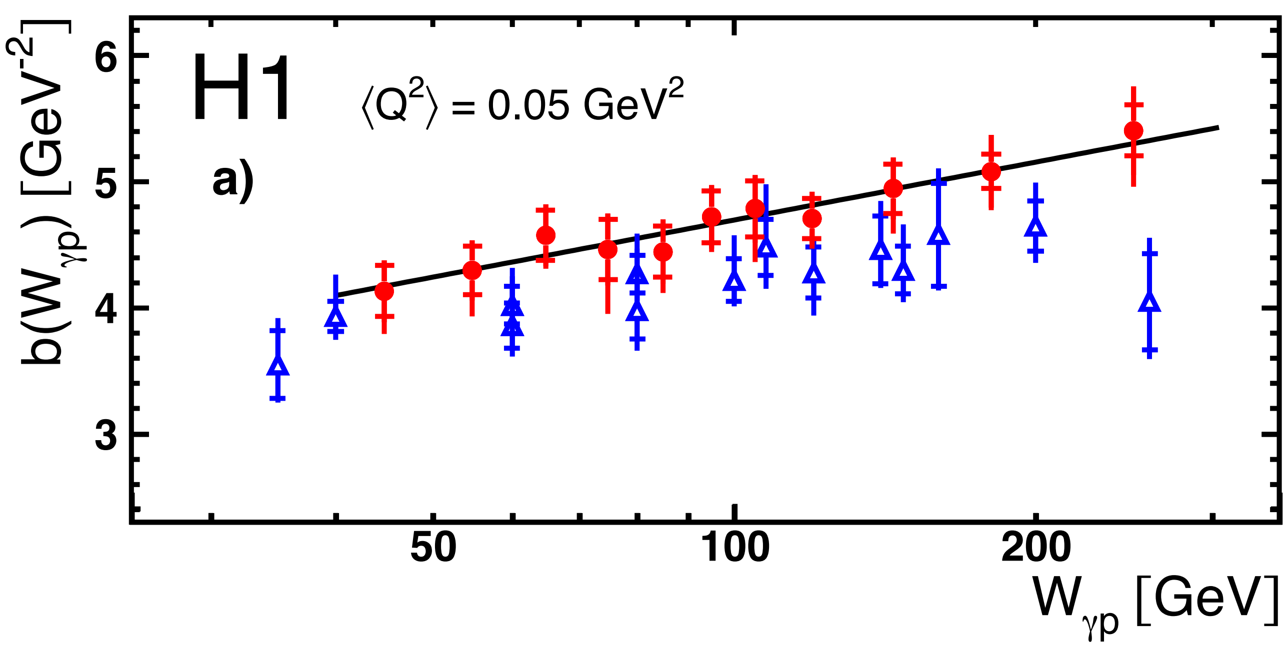

The slope growths with energy:

$$b(W) = b_0 + 4\alpha' \ln(W_{\gamma p}/W_0)$$

Growth of the target size with energy

Small energy

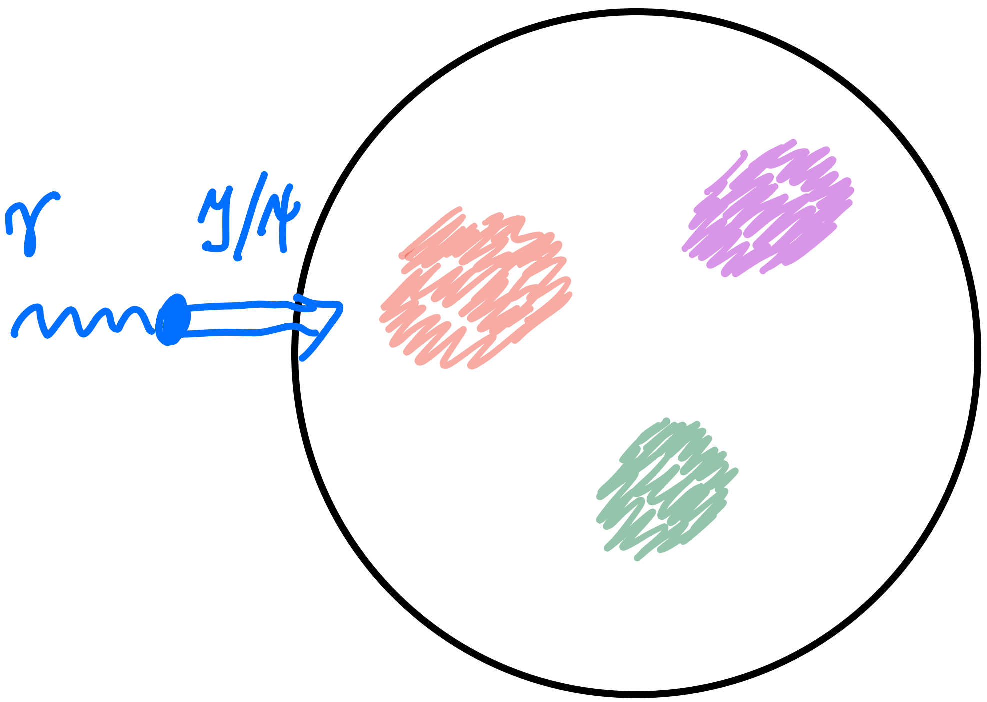

Target

Large energy

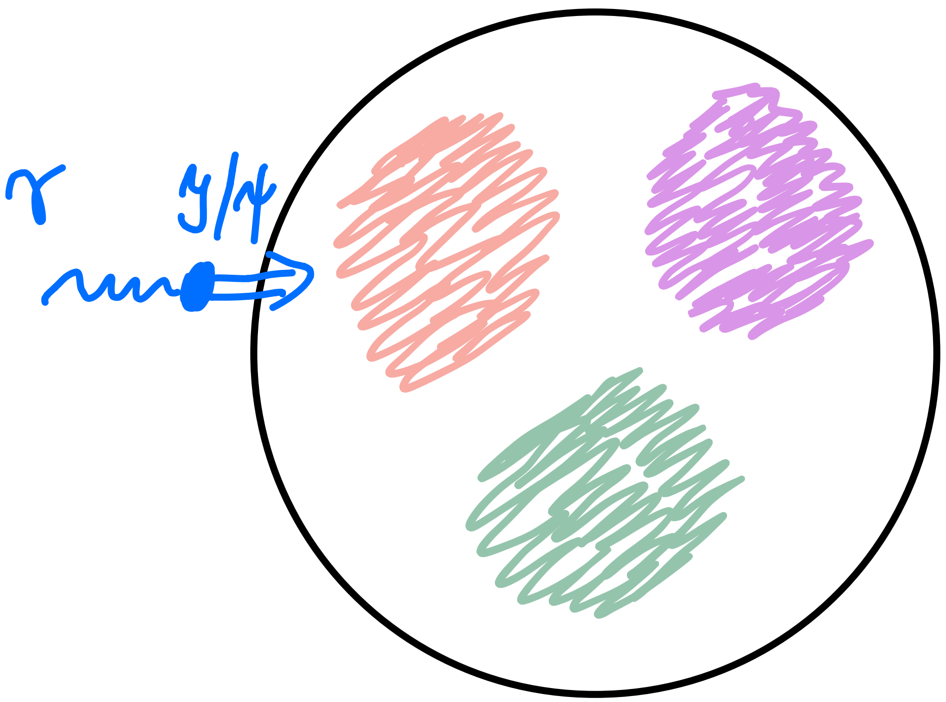

Target

The target size, i.e. the region of gluon density probed by the vector meson increases with energy

Elastic vector meson production at EIC

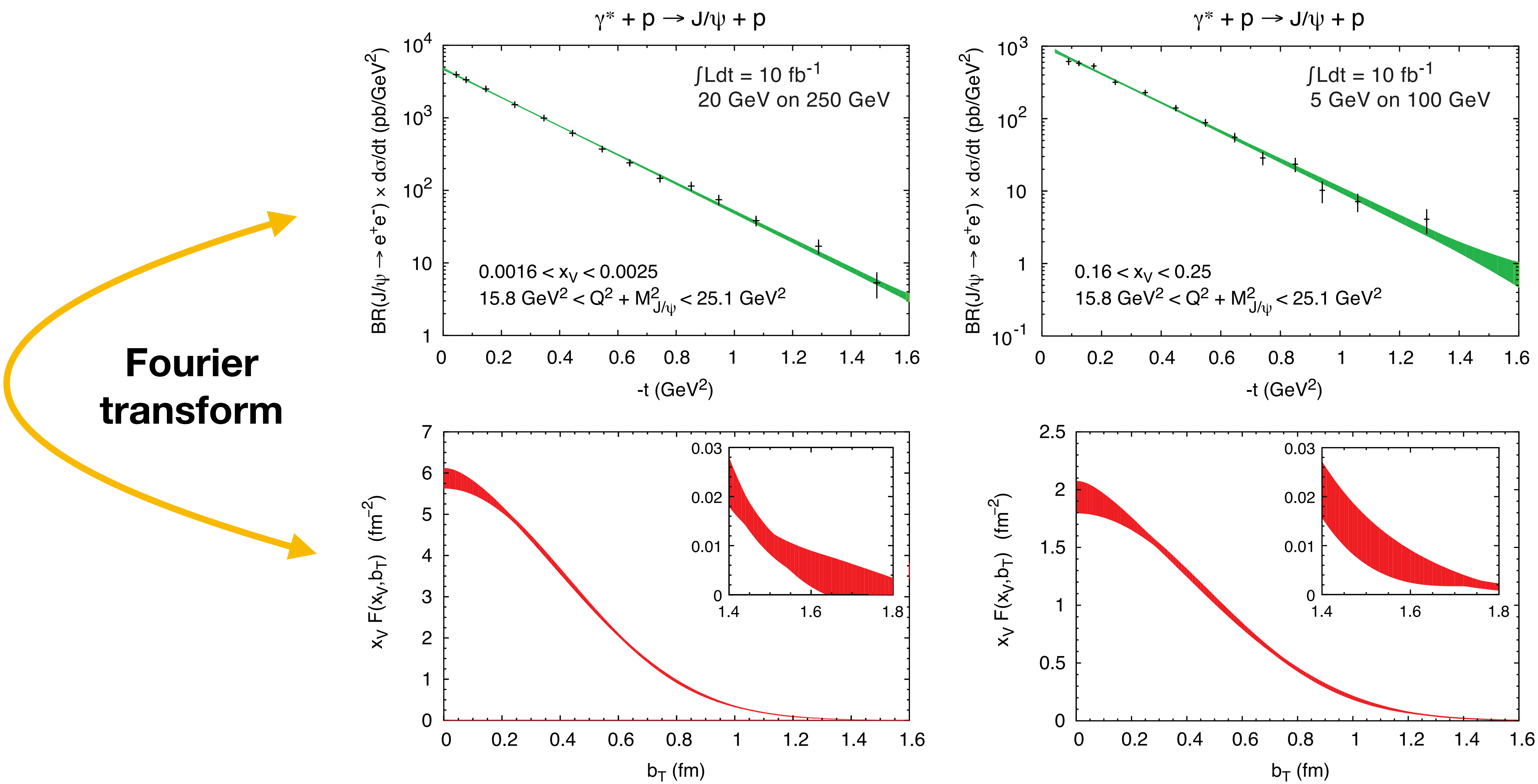

EIC, White paper

EIC: lower energy than HERA, different kinematics.
Very high statistics, high precision

Profile function from elastic vector meson production

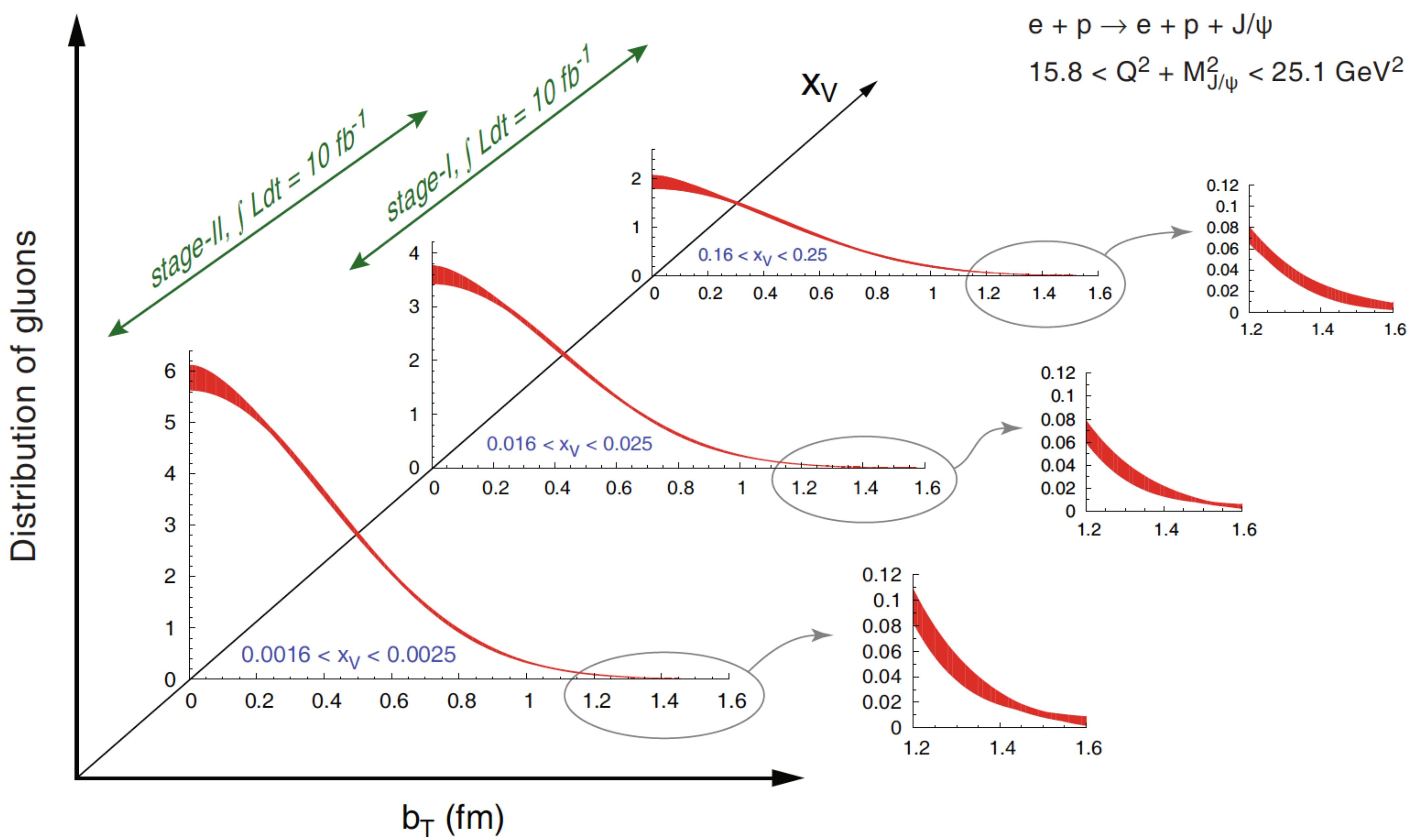

Elastic vector meson production at EIC : eA

EIC, White paper

Nuclear target: Au

$$e + Au \to e + Au + J/\psi$$

Characteristic 'dips' in t-distribution

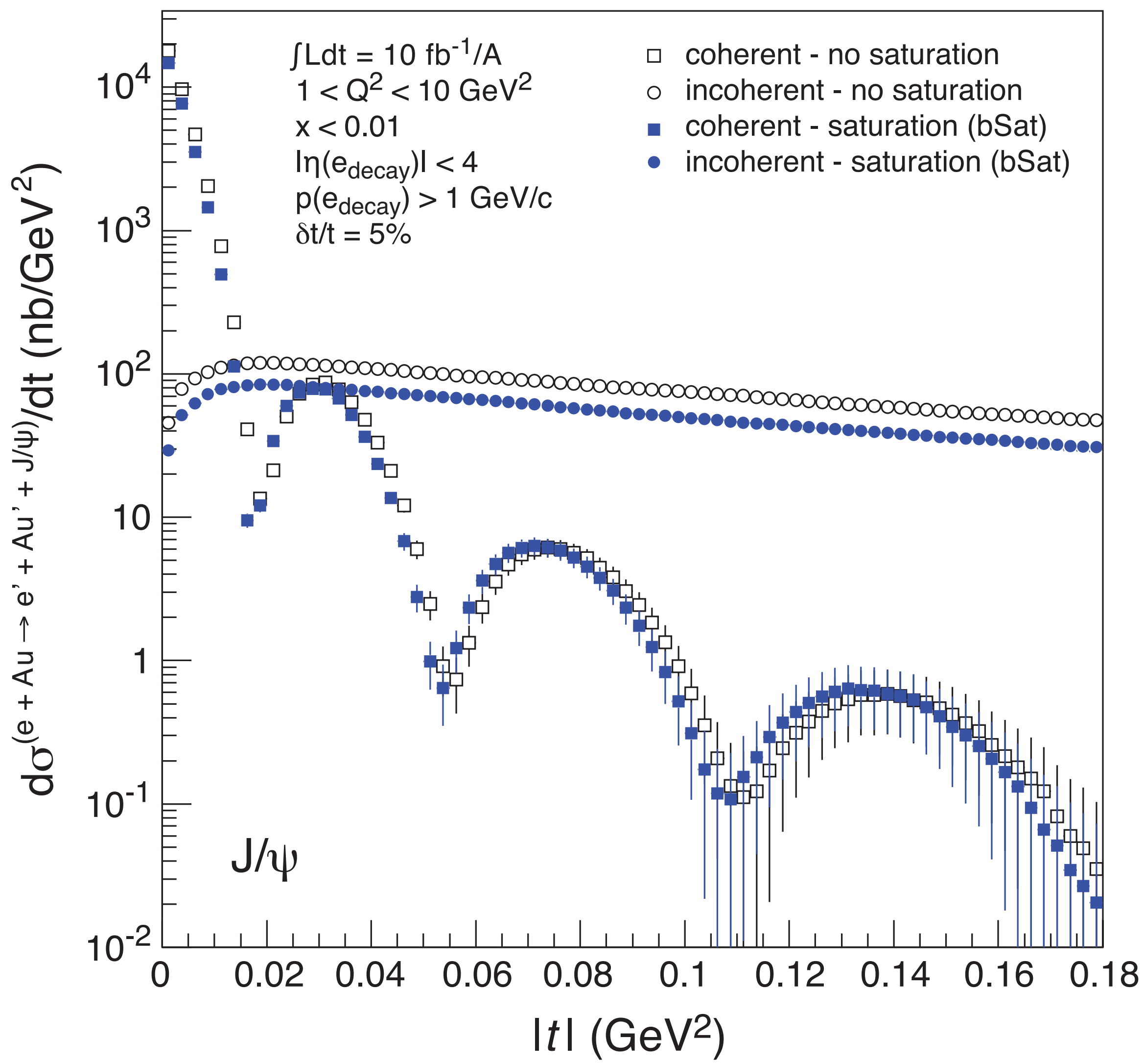

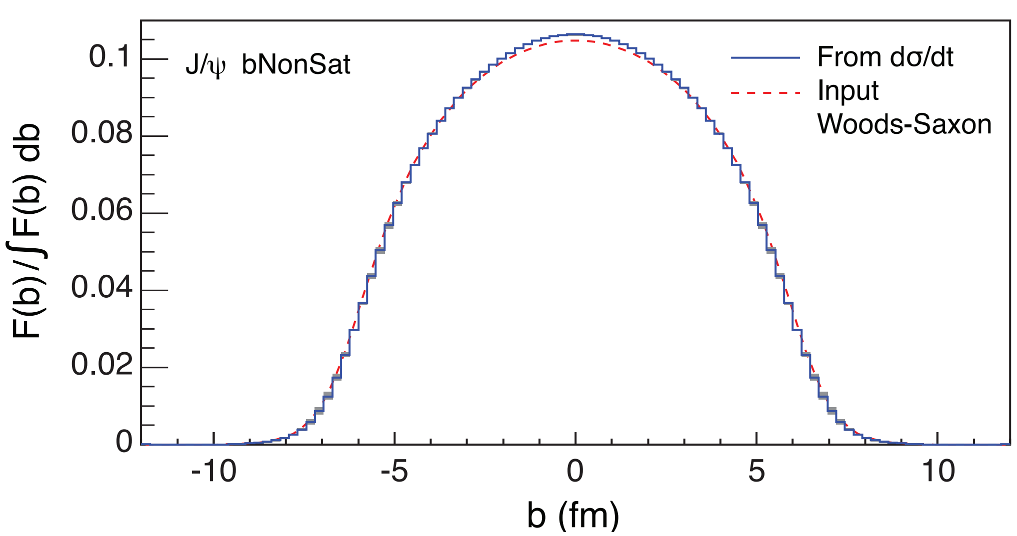

$$F(b) = \int_0^\infty \frac{q\,dq}{2\pi} J_0(qb) \sqrt{\frac{d\sigma_{\text{coherent}}}{dt}}$$

$$t = -q^2$$

Coherent vs incoherent

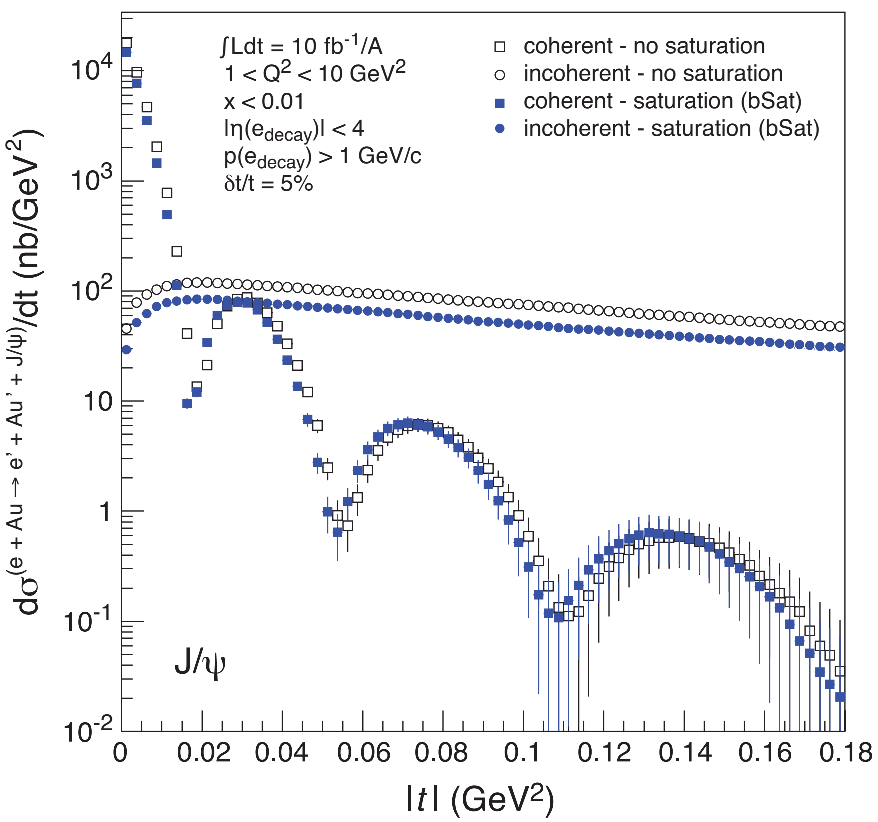

Coherent:

Depends on the shape of the source, average distribution

Incoherent:

Provides information about the fluctuations or lumpiness of the source

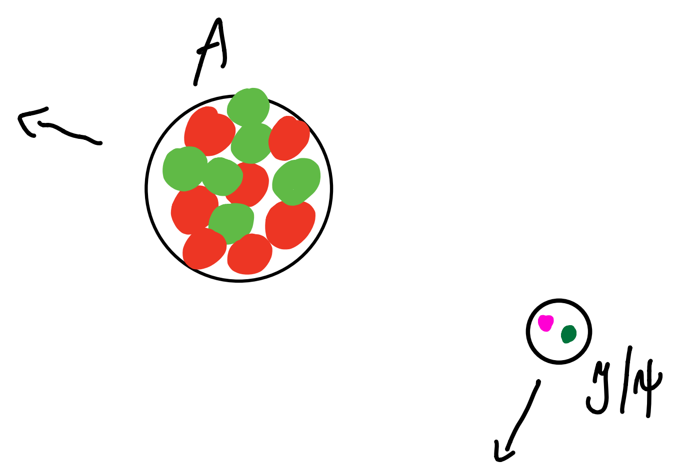

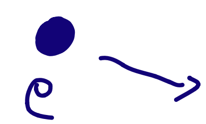

Coherent
(Nucleus stays intact)

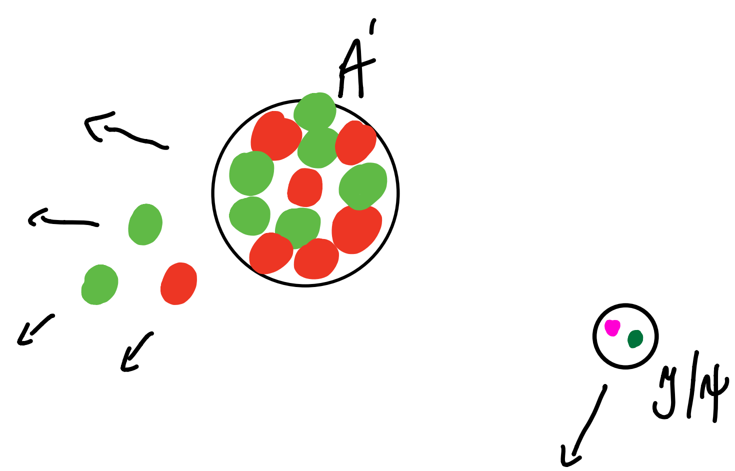

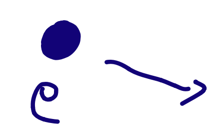

Incoherent
Nucleus breaks up

Diffractive J/ψ in electron-deuteron

Diffractive J/ψ scattering on a deuteron as a way to study short - range correlations (SRC)

Short-range correlated nucleon pairs with high internal nucleon momentum (quasi-deuteron inside the nucleus). Possible strong link of SRC to EMC effect.

Questions:

- Role of gluons in SRC pairs?
- Relation of SRC to shadowing and/or saturation ?
- Spatial and momentum distribution of partons in high momentum configurations ?

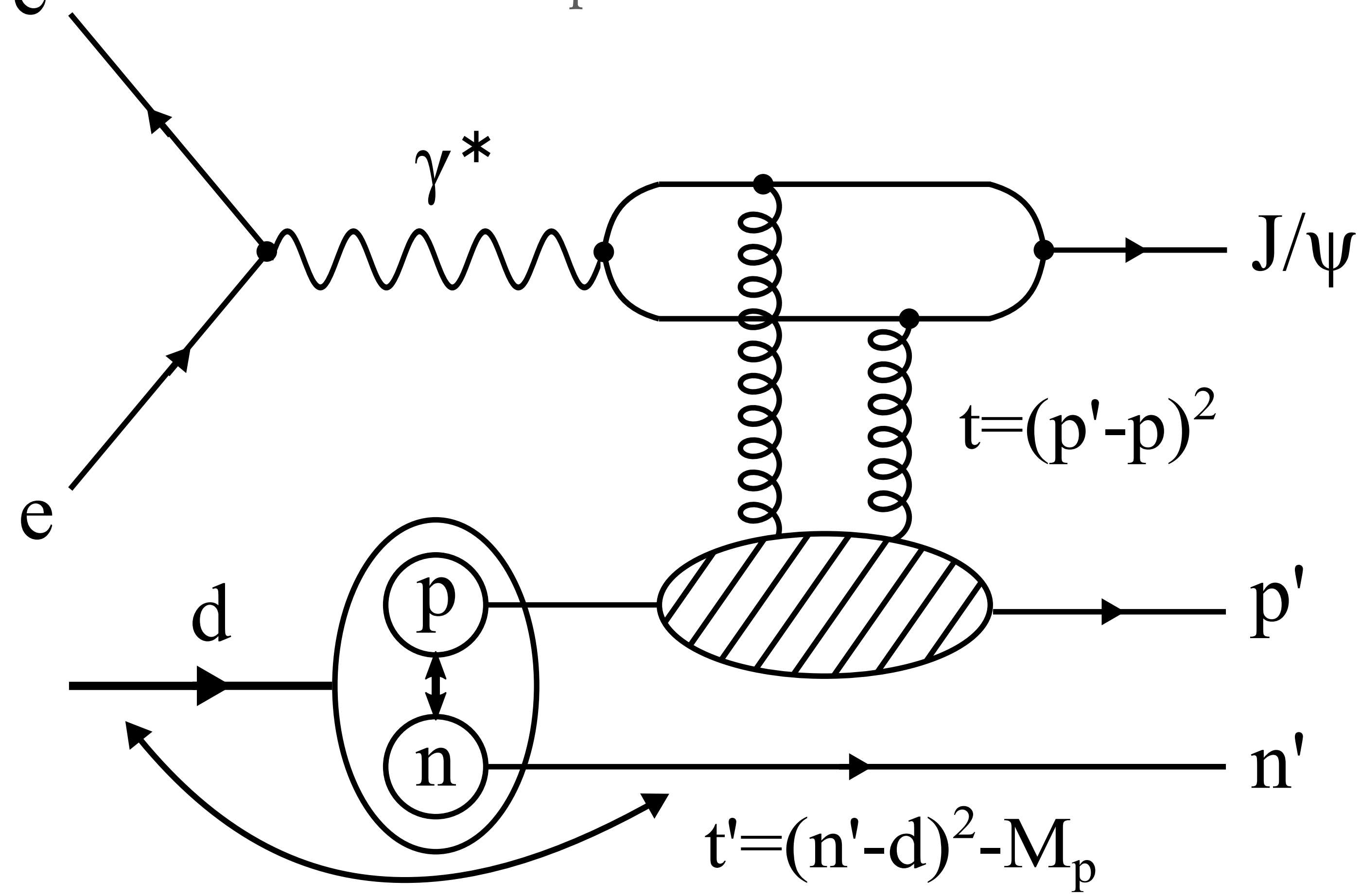

Momentum transfer t, the difference between outgoing proton momentum and incoming proton momentum, which is not known in ed, unlike in ep

$$t = (p' - p)^2$$

Reconstruction of t : through leading nucleon and spectator measurement (proton and nucleon are back-to-back in the rest frame of pn before the interaction)

$$t = (p' - (-n))^2$$

Distribution in t for diffractive J/ψ in electron-deuteron

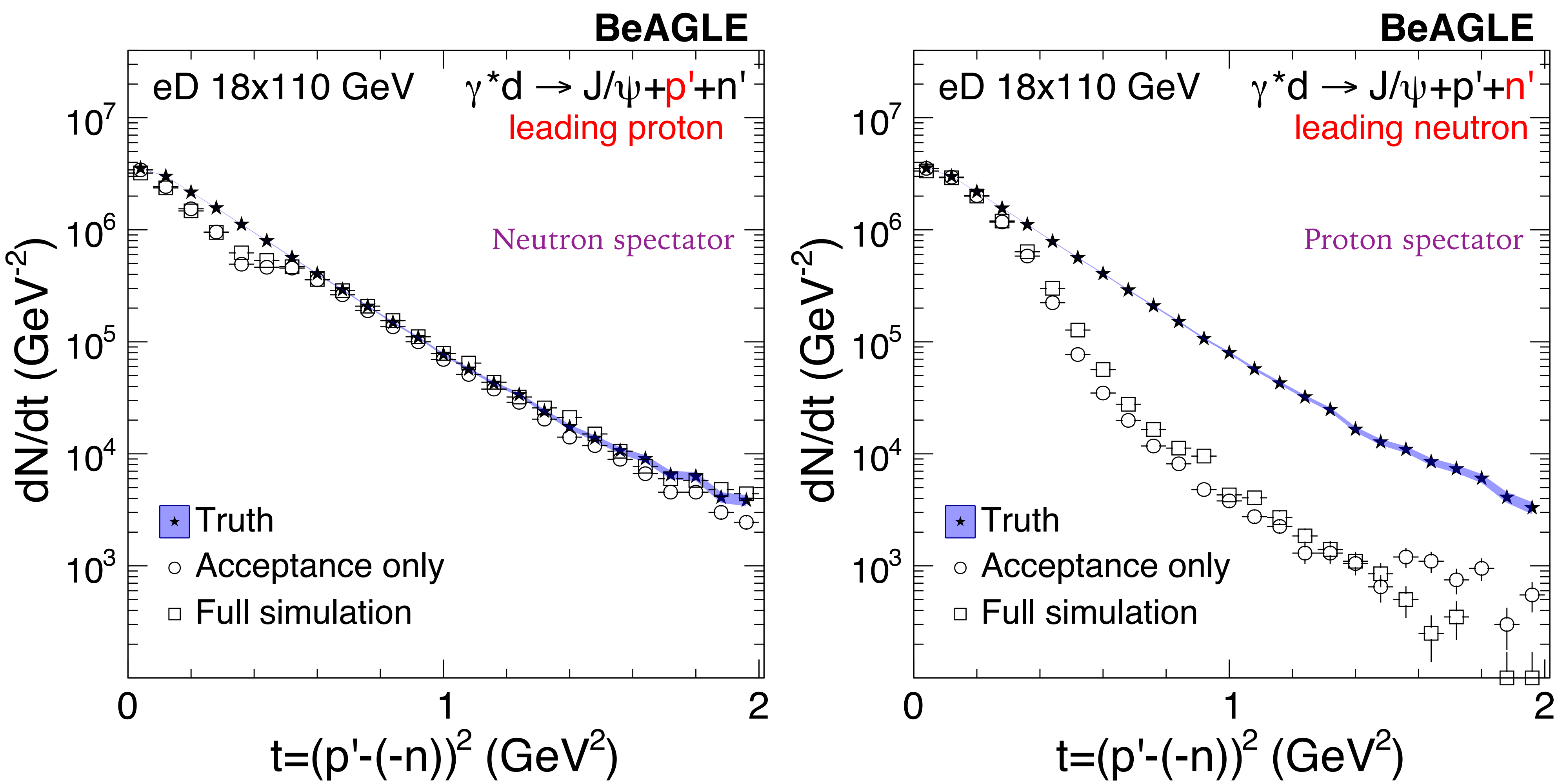

Integrated over a range of p_m

Method requires double tagging of both proton and neutron

In general t distribution affected by acceptance and resolution of nucleons

Good precision in neutron spectator case

Summary

EIC offers ample opportunities for studying diffraction and forward physics

Excellent proton and neutron tagging capabilities, precision measurement of diffractive structure functions, Pomeron/Reggeon

Prospects for F_L^D and 4-dim structure function

Nucleon/nuclear imaging with diffractive vector meson production

Study of SRC with EIC

Diffractive production off light nuclei, double spectator tagging in light nuclei

…and much more!

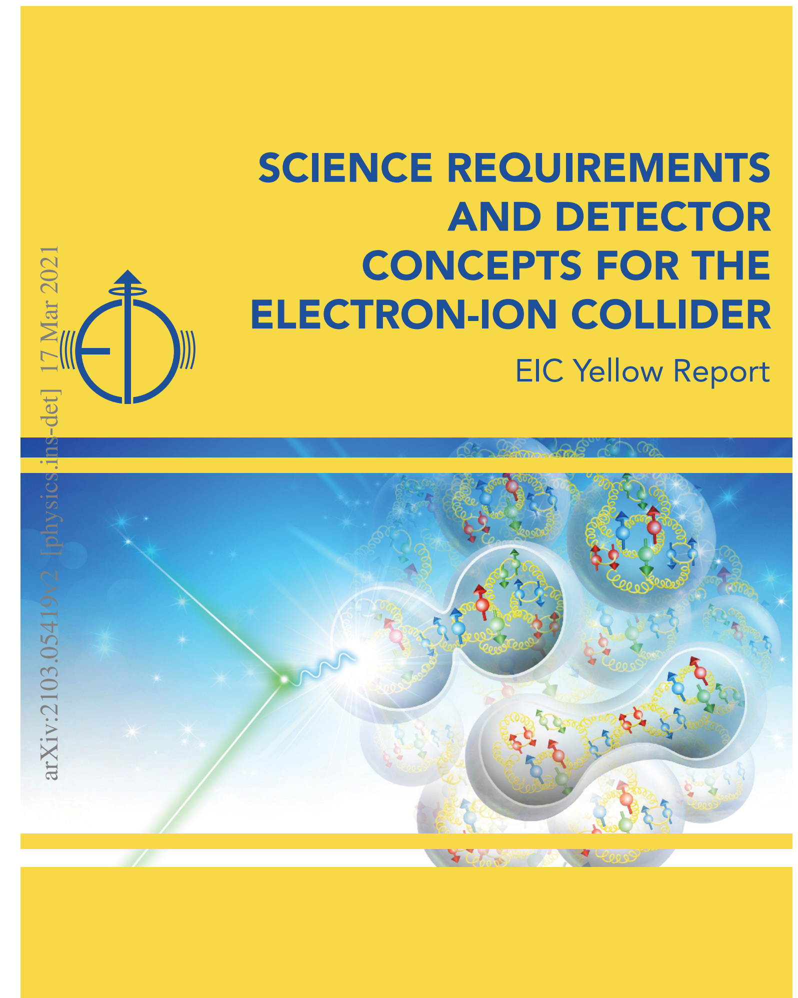

Yellow Report

arXiv:2103.05419

Thank you!